POLITECNICO
MILANO 1863

SCUOLA DI INGEGNERIA INDUSTRIALE
E DELL'INFORMAZIONE

Control and Simulation of Steel Strips in Galvanization Lines

Tesi di Laurea Magistrale in
473 Engineering - Ingegneria dell'Automazione

Author: **Enrico Tranquillini**

Student ID: 951269
Advisor: Prof. Gianni Ferretti
Co-advisors: Luca Bascetta
Academic Year: 2022-23

Abstract

Hot-dip galvanization is an industrial process involving the application of a uniform coating of zinc to steel strips with the desired thickness. Disturbances from air knives and external factors during the galvanization process can lead to deviations in the strip's path, resulting in an uneven layer of zinc. To achieve a uniform coating, it is essential to minimize the strip's vibrations by implementing effective stabilization measures.

The overarching aim of the research is to establish a user-friendly tool for efficiently simulating and predicting the behavior of strips made from various materials, with different lengths and widths. In this thesis, a new mathematical model has been developed to predict the vibrations of a steel strip during the hot-dip process.

The model is based on the Finite Element Method (FEM), and its validity has been confirmed through data acquired from an operational plant. Several alternative methods were investigated in the pursuit of model development, such as Recursive Least Squares (RLS), time series, and Differential Algebraic Equations (DAE) with an acausal approach.

Following the model development, a controller is designed to stabilize the vibrations of the strip. Previous controllers utilized PID and PLC to control the position of steel strips. The new controller utilizes a pole placement technique with a state observer, testing has been confined to simulation. The control strategy is specifically crafted to operate on the natural frequencies of the steel strip, leaving other frequencies unaffected.

The findings indicate that the model can effectively estimate natural frequencies for the steel strip based on its mechanical parameters and dimensions, aligning with experimentally identified modes. The Finite Element Method is employed to calculate the Frequency Response Function (FRF) of the strip on specific positions along the strip, and then simulate the process. Knowledge of the FRF Through simulation testing, the controller demonstrates its efficacy in stabilizing the strip's vibrations at specific frequencies. The use of an observer is instrumental in this success, compensating for the unmeasurable nature of the states.

Keywords: Hot Dip Galvanization, Pole Placement

Abstract in lingua italiana

La zincatura a caldo è un processo industriale che prevede l'applicazione di uno strato uniforme di zinco su nastri di acciaio dello spessore desiderato. Durante il processo di galvanizzazione, le perturbazioni causate dai coltelli d'aria e da fattori esterni possono provocare deviazioni nel percorso del nastro, con il risultato di uno strato di zinco non uniforme. Per ottenere un rivestimento uniforme, è essenziale ridurre al minimo le vibrazioni del nastro implementando misure di stabilizzazione efficaci.

L'obiettivo principale della ricerca è quello di creare uno strumento di facile utilizzo per simulare e prevedere in modo efficiente il comportamento di nastri realizzati con vari materiali, di diverse lunghezze e larghezze. In questa tesi è stato sviluppato un nuovo modello matematico per prevedere le vibrazioni di un nastro di acciaio durante il processo di zincatura a caldo.

Il modello si basa sul metodo degli elementi finiti (FEM) e la sua validità è stata confermata dai dati acquisiti da un impianto operativo. Per lo sviluppo del modello sono stati studiati diversi metodi alternativi, come i minimi quadrati ricorsivi (RLS), le serie temporali e le equazioni algebriche differenziali (DAE) con un approccio acausale.

Dopo lo sviluppo del modello, è stato progettato un controllore per stabilizzare le vibrazioni della striscia. Il controllore utilizza una tecnica di posizionamento dei poli con un osservatore di stato. I test sono stati limitati alle simulazioni. La strategia di controllo è stata studiata per operare sulle frequenze naturali del nastro d'acciaio, lasciando inalterate le altre frequenze.

I risultati indicano che il modello è in grado di stimare efficacemente le frequenze naturali del nastro d'acciaio in base ai suoi parametri meccanici e alle sue dimensioni, allineandosi con i modi identificati sperimentalmente. Il metodo degli elementi finiti viene impiegato per calcolare la funzione di risposta in frequenza (FRF) del nastro in posizioni specifiche lungo il nastro e successivamente simulare il processo. Attraverso test di simulazione, il controllore dimostra la sua efficacia nello stabilizzare le vibrazioni della striscia a frequenze specifiche. L'uso di un osservatore è determinante per questo successo, in quanto compensa la natura non misurabile degli stati.

Parole chiave: Zincatura a caldo, posizionamento dei poli

Contents

1 | Introduction

In the industrial landscape, galvanized steel strips play a pivotal role, serving as a cornerstone for a myriad of applications ranging from construction to automotive industries. The galvanization process, involving the application of a protective zinc coating to steel, enhances the material's corrosion resistance and durability, thus expanding its utility and lifespan.

As demands for high-quality galvanized steel continue to grow, understanding and optimizing the galvanization process is of paramount importance to meet stringent quality standards and economic efficiency. An important aspect of the galvanization process is the zinc coating's uniformity, which is crucial for the material's performance and longevity in any environment.

An excessive amount of zinc can lead to an uneven coating, resulting in a rough surface and increased material usage. Conversely, insufficient zinc can lead to corrosion and rusting, compromising the material's integrity. Therefore, it is essential to achieve a uniform coating of zinc to ensure the material's quality and durability.

In the past decades, numerous approaches have been proposed for the design of an efficient control of the galvanization process.

Recent technological advancements have introduced new types of sensors and actuators into the galvanization process, enabling the exploration of innovative control strategies.

In the historical context, the control of steel strip vibrations relied exclusively on air knives to avoid any direct physical contact with the strip, which could compromise its integrity. This constraint imposed limitations on the types of actuators and sensors applicable to this specific application. When relying solely on air knives, control over strip vibrations faced several challenges: lack of strip positional information, the use of outdated sensors resulted in insufficient information regarding the positional state of the strip. Sudden changes in strip speed introduced varying measurement time delays, complicating the control process. Absence of air Knife position skew controllers and The lack of controllers for adjusting the position of air knives led to non-uniform air flow, contributing to irregularities in the

deposited zinc layer.

These limitations underscored the need for advancements in sensor and actuator technologies, prompting the exploration of new control strategies to address these challenges and enhance the galvanization process. The most promising of these technologies has been the usage of a magnetic stabilization systems. This system is composed a series of electromagnets positioned on both sides of the strip. Based on the fed current, they apply an attractive force to the strip, pulling in the strip from one side or the other. This system is capable of providing a more accurate control of the strip's vibrations, as it can be adjusted to the strip's position and speed.

The prevailing literature and current methodologies for controlling the galvanization process primarily rely on PID controllers implemented in both magnetic and air knife stabilization systems. While PID systems excel in managing predominantly linear systems and known dyanmics, as we will elucidate, steel strip vibrations at higher frequencies can only be accurately described by a nonlinear model.

The analysis of PID controllers reveals their proficiency in tracking and controlling signals; however, their efficacy is challenged in the context of the galvanization process due to its unpredictable system evolution. The inherent time delay between input and output amplifies these challenges, particularly when dealing with the nonlinear dynamics of steel strip vibrations.

This thesis embarks on a comprehensive exploration of galvanization processes, with a specific focus on applications involving steel strips. The study aims to deeply investigate the intricacies of the galvanization process, encompassing underlying principles, techniques, and factors influencing the quality of the zinc coating. Furthermore, it seeks to integrate advanced methodologies, including computational simulations and empirical analysis, to optimize the galvanization process for steel strips.

The primary objective of this research is to enhance the production of galvanized steel strips by gaining a comprehensive understanding of the dynamics governing the vibrations and subsequently controlling them. The ultimate goal is to achieve a uniform, high-quality zinc coating.

By unraveling the fundamental principles shaping the galvanization process and employing state-of-the-art analytical tools, this study aspires to offer valuable insights and recommendations. These contributions are intended to advance galvanized steel strip production, fostering sustainability and innovation within the industry.

In Chapter 1, we will provide a concise overview of the galvanization process, delving into

its historical background and diverse sections. This chapter will also address the primary challenges associated with the process, outlining the main actuators, disturbances, and prevalent control strategies employed in the industry.

Moving on to Chapter 2, our focus will be on delineating the principal mathematical models utilized in the literature to elucidate the vibrations of steel strips, elucidating their key characteristics.

In Chapter 3, we will expound on the acquisition process of data from an actual plant and detail the subsequent data processing procedures.

Chapter 4 will be dedicated to outlining the methodology employed in calculating the Frequency Response Function (FRF), with a specific emphasis on the application of the Finite Element Method (FEM) to compute the FRF of the steel strip.

Chapter 5 will delve into the description of the control scheme, featuring the adoption of a pole placement technique in conjunction with a state observer. Notably, the testing of this control strategy has been limited to simulations, and the approach is meticulously designed to target the natural frequencies of the steel strip while leaving other frequencies unaffected.

2 | Process Description

2.1. Hot Dip Galvanization

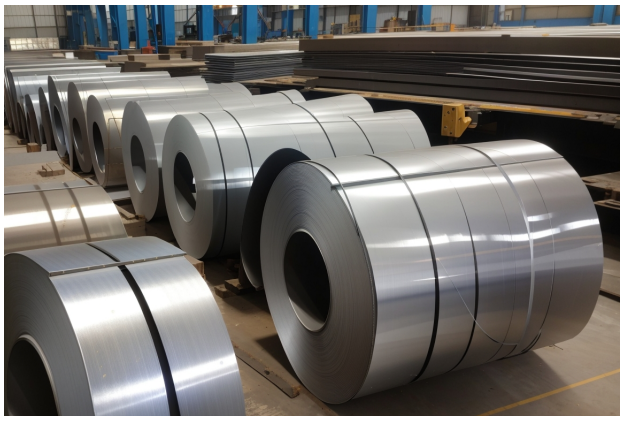

Figure 2.1: Steels strips - galvanized product

Hot-dip galvanization is an industrial process that entails immersing a specific product into a pool of liquid zinc. The primary objective of this procedure is to safeguard the product from corrosion caused by environmental factors. The end product are steel strip plates which are used in a variety of applications, such as automotive, construction, and manufacturing industries.

This chemical treatment ensures low maintenance or even maintenance-free corrosion protection, effectively shielding against natural elements, preserving value, and improving overall quality of life of the product.

Corrosion protection is achieved through the application of protective layers, effectively isolating the metal material from corrosive agents. These protective layers can be applied to steel products using various methods, such as wire galvanizing, tube galvanizing, or wire spraying galvanizing.

There are several types of hot dip galvanization methods, such as batch galvanizing, tube galvanizing, wire galvanizing, sheradizing and spraying galvanizing, each with its own advantages and disadvantages. These vary from the size of the product, the thickness of

the coating, the speed of the process, the cost of the process, the quality of the coating and the different shapes of the product to be galvanized.

Within the scope of this thesis, our emphasis is placed on continuous sheet galvanizing, specifically continuous hot-dip strip galvanizing, as the preferred method. This choice is motivated by our work with thin mild steel strips. This method ensures a consistent and high-quality protective coating. Understanding the nuances of this process is vital for comprehending the potential advantages and limitations it offers in terms of corrosion protection and its implications for the industry.

2.1.1. Continuous Hot-Dip Galvanizing Line

Continuous hot-dip galvanization follows these main steps:

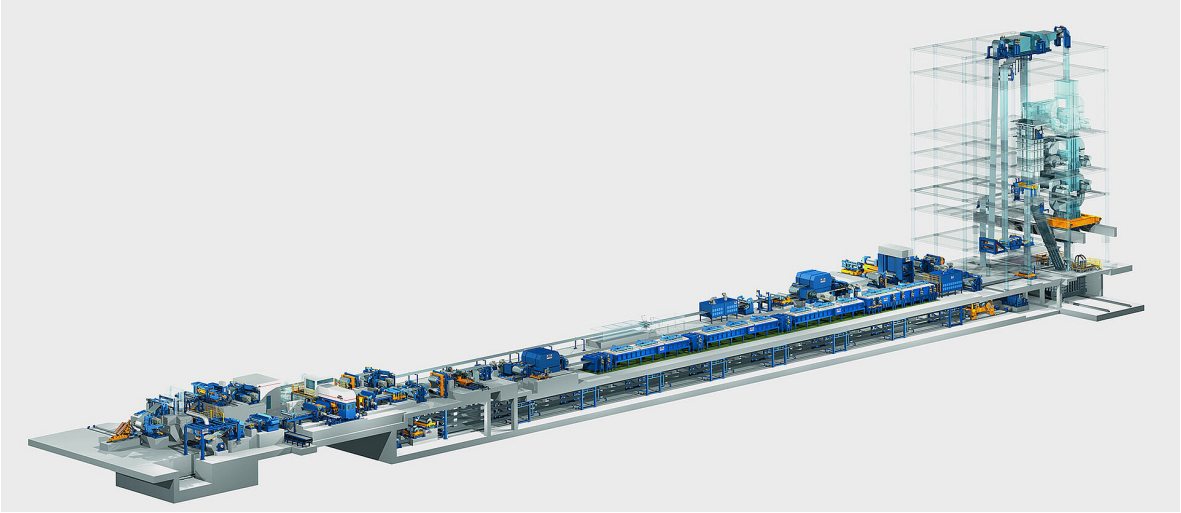

Figure 2.2: Continuous hot-dip galvanizing line general scheme

The inputs are rolls of steel sheets or plates which are unrolled and fed into the galvanization line. The steel strip is then processed through a series of steps, which are:

1. **Pre-Cleaning:** Steel or iron products are first thoroughly cleaned to remove any dirt, grease, oil, or other contaminants. This step is crucial to ensure good adhesion of the galvanized coating on the final product.
2. **Degreasing:** Products are immersed in a degreasing solution to remove any remaining grease or oils.
3. **Pickling:** The products are then immersed in an acidic solution (typically hydrochloric acid) to remove rust, mill scale, and other impurities from the surface.

Pickling creates a clean and chemically active surface.

4. **Fluxing:** After pickling, the products are dipped in a flux solution (usually a mixture of zinc ammonium chloride) to promote uniform coating and enhance the adhesion of the zinc during galvanizing.
5. **Galvanizing Bath:** The cleaned and fluxed products are immersed into a bath of molten zinc at a high temperature (around 450° C to 460° C). The high temperature allows the zinc to bond metallurgically with the steel or iron, forming a zinc-iron alloy layer.
6. **Cooling:** After galvanizing, the products are slowly withdrawn from the zinc bath and allowed to cool in the air or in a quenching bath to solidify the zinc coating.
7. **Inspection and Quality Control:** The galvanized products are inspected for coating thickness, uniformity, adherence, and overall quality to ensure they meet the specified standards and requirements.
8. **Drying and Curing:** The galvanized products may undergo a drying process to remove excess moisture and ensure the coating is properly cured and hardened.
9. **Finishing and Packaging:** Depending on the application and requirements, the galvanized products may undergo additional processes such as passivation, chromating, or painting for enhanced corrosion resistance or improved aesthetics. After this, the products are packaged and prepared for distribution or further use.

This thesis focuses around the **coating segment of the process**, which has equal importance as many other segments now described, but little delays or excessive vibrations in this segment can cause a bottleneck for the entire process.

2.1.2. Coating Segment

Let's describe into more detail the coating segment of the hot dip galvanization process. The following picture shows it in a simplified manner:

Concentrating on this specific segment of the process, the mild steel strip is projected forward via motors through a series of rollers, which guide it into different directions. Several rollers place the strip into descending direction as seen in figure (a), coming from an annealing furnace. The strip is immersed into a pool of liquid zinc where it forms an inter-metallic layer with the steel when they are in contact at high temperatures at around 450° C. Following that, the bottom roller guides the strip vertically, while the correction

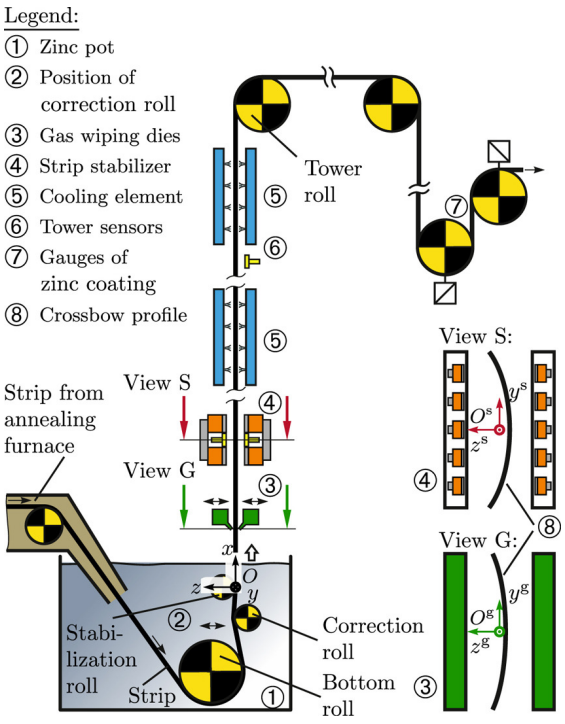

Figure 2.3: *Coating Segment[2]*

rollers ensure that the strip moves in the correct vertical direction. Its verticality allows excess zinc to flow into the pool uniformly without loss of material. Though the strip is now covered in zinc, a specific thickness of said layer is an important parameter to consider for an optimal result.

A minimum thickness is required by industrial standards to protect the steel from external contagious elements, and a maximum thickness is a necessity not only for economic purposes, since zinc is an expensive material in liquid form, but also for the weight of the final product.

In this vertical section, the steel strip is moving at a certain speed and a series of air knifes push a stream of pressured air on the strip in order to remove any liquid zinc in excess. This also aim to shape a uniform layer of zinc on the strip, usually as thin as $60\mu m$. This will be considered as our primary disturbance, which we will dwell deeper later. The air knives shoot pressured air from both sides cycling in accordance with a switching system. Here we are arriving to the main point of this thesis. While the strip undergoes a vertical movement, it also undergoes a longitudinal movement due to the air knifes and other minor factors which will be described afterwards.

The crucial factor is the longitudinal position of the strip in relation to its equilibrium position. This stability not only constrains the speed at which the line can operate but

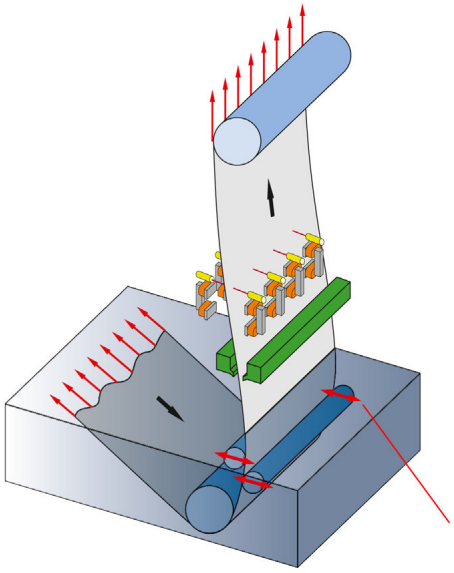

Figure 2.4: *Rollers[6]*

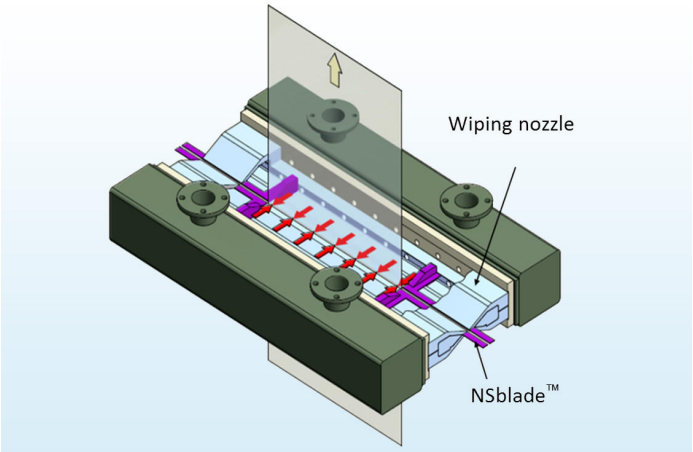

Figure 2.5: Air knife, the main source of the vibrations

also significantly impacts the quality of the final product. It's evident that a more stable strip allows for a more uniform coating, contributing to an overall improvement in the final product. Moreover, a faster production line translates to a higher output of finished products, thereby bolstering company profits in the long run. Consequently, the task of ensuring strip stability is of paramount importance.

Historically the air knifes were used both as actuators to stabilize the strip and to remove excess zinc. However, this approach proved to effective, but with constraints on the thickness of the zinc layer. To address this issue an emerging standard practice is to utilize an **electromagnetic strip stabilizer**. Electromagnetic coils generate controlled magnetic fields which interact with the steel strip, exerting an attractive force, minimizing

lateral movement, and counterbalancing external disturbances. Magnetic forces stand out as the current solution, as they possess the capability to counteract vibrations at high frequencies without physically contacting the strip, thereby avoiding any alteration to the coating.

Figure 2.6: Electromagnetic Stabilizers using DC

Many inductive displacement sensors are used to measure the distance of the steel strip from a fixed position, which is the sensor's position. It does so by generating an electromagnetic field, same in nature as the stabilizers, and detecting changes in inductance caused by variations of the distance between the sensor and the target.

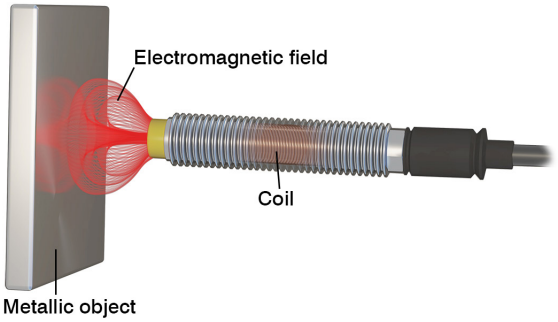

Figure 2.7: Inductive Sensors, magnetic field generated by the coil

Afterwards the strip undergoes controlled cooling, solidifying the zinc coating through another series of cooling jet streams of air. While the cooling progresses, the galvanized strip may be further treated to ensure an even surface. It's then inspected for coating thickness, uniformity, and overall quality. Any necessary adjustments or corrections may be made at this stage.

2.2. Importance of the Electromagnetic Stabilizer

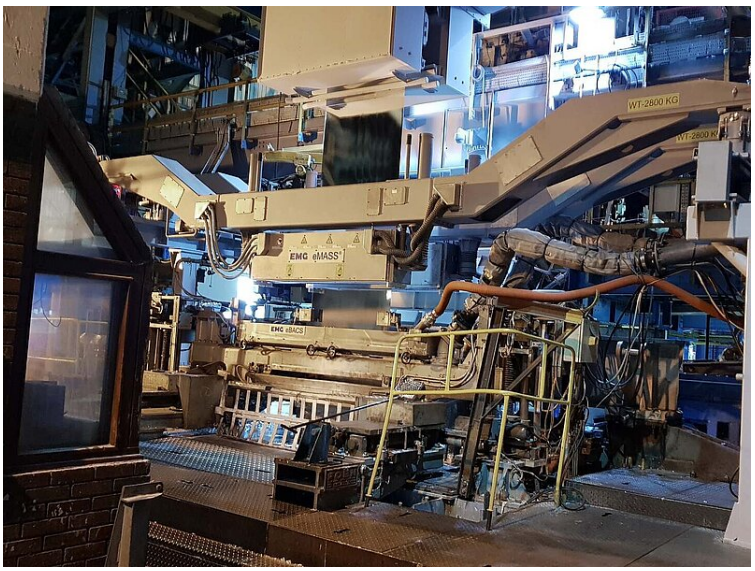

Figure 2.8: Electromagnetic Stabilizer structure - External view

The previous literature and the current standard of magnetic stabilizers had the main purpose of controlling the system based on the known disturbances. These known disturbances are associated to mechanical component, such as the rollers which direct and correct the flow of the strip. Previous controls in industry are able to handle this known disturbances at low frequencies between 0 and 10 hertz with classic control algorithm.

Our scope is to tackle the **unknown disturbances**, whose source will be explained later. The main concept to keep in mind is these disturbances have lower magnitude but spread on a wider frequency spectrum. For these vibrations the sources magnitude and frequencies are unknown, so we will use a white noise excitation to simulate this kind of interfences. They are most likely impulses which then excite the resonance frequencies of the strip, which cause the perturbations we observe.

2.2.1. Source of the Vibrations

The source of the vibrations are:

- Air knifes: known disturbance, but not controllable since they serve to uniform the zinc layer
- Rotation of the mechanical parts, specifically the rollers: known frequencies since mechanical properties and dimensions are known

- External disturbances from environment: unknown frequencies, not controllable

Since the mechanical frequencies are known, a control action has already been developed and deployed to counteract vibrations of this kind. This control action is a PID (Proportional-Integral-Derivative) controller, included in the galvanization line thorough PLCs.

Danieli Automation has developed an architecture with electromagnets which is able to counteract these vibrations at higher frequencies, but it is not able to control the strip at a high frequency. The main reason is that the control action is based on a model which is not able to explain accurately the behavior of the strip at a higher frequency. This unique application has 2 different distinguished components:

- Electromagnetic coils based on DC (Direct Current) component which can be used to generate a magnetic field in order to control vibrations at a low frequency, targeted an known inputs.
- Electromagnetic coils based on AC (Alternate Current) component which can be used to generate a magnetic field in order to control vibrations at higher frequencies, for unknown elements.

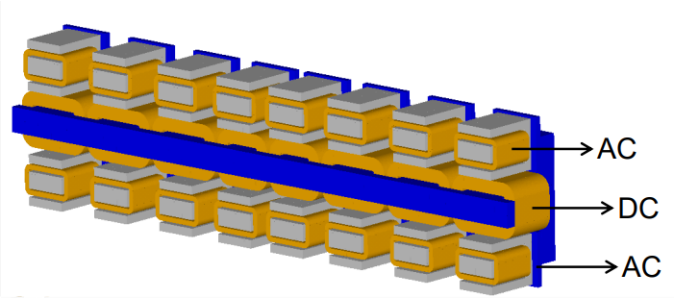

Figure 2.9: Danieli Electromagnetic Stabilizer

The emerging frontier lies in the control of vibrations at high frequencies, as these can be elucidated using more intricate models. In the contemporary industry, steel sheets and plates exhibit variations in width, thickness, length, and diverse chemical and physical properties. Vibrations at higher frequencies, particularly those originating from unknown sources, trigger resonance frequencies in steel strips based on their mechanical and physical characteristics. The ability to create a simulated environment for developing a specific control strategy tailored to any type of strip holds the potential to significantly reduce costs and production line time.

In configuring these industrial lines, numerous variables and elements must be considered for a specific strip. Some parameters rely on experience, while others are fine-tuned during the initial production phase. Simulated environments prove invaluable in minimizing the duration of initial production and cutting down on production line costs.

Presently, there are models capable of interpreting data acquired from high-frequency vibrations, employing nonlinear models. However, these models often sacrifice simplicity in application. Consequently, we will initially explore a linear approach, seeking a technique that is more easily applicable.

3 Theory of Vibrations

3.1. Theory Vibration and Modal Analysis

3.1.1. Representations

There are different ways to represent a mechanical vibrating system. We will treat and use each of these representations in this thesis, since each of them has its own uses.

Spatial Representation

- M is the mass matrix
- K is the stiffness matrix
- C is the damping matrix

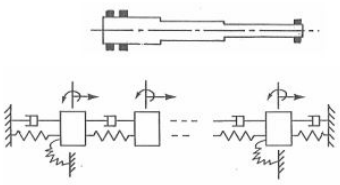

Figure 3.1: Spatial representation of the system

The matrices are in the form of NxN, where N is the number of degrees of freedom of the system, as well as the number of equations of motion. The representation sees the system as a series of mass connected via dampers and springs.

Modal representation

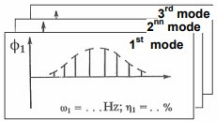

Figure 3.2: Modal representation of the system

- $[\lambda]$ .. spectral matrix, diagonal, eigenvalues are on the diagonal
- $[\Phi]$ .. mode shape matrix, columns are the modal shapes

Frequency representation

- $H(\omega)$..frequency response function matrix

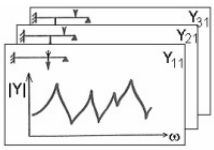

Figure 3.3: Frequency representation of the system

Each of these will have its different scopes:

- Spatial representation: for the computation and simulation of the system
- Modal representation: for the validation of the identified model and the comparison with the spatial representation
- Frequency representation: for the Identification of the modal frequencies from data.

3.1.2. Vibrations and Modal approach

Our goal is to develop our mathematical model which explains how the steel strip vibrates longitudinally in response to a certain disturbance, and then simulate it via a Finite Element Method. This method is a widespread in the industry to simulate complex geometries with limited computational complexity, without requirements on complex software and easily explainable to the engineers.

Firstly to understand the external disturbances we need to understand how vibrations work and their sources. Vibration is a repetitive motion of an object around an equilibrium point. For a general mechanical system composed of n body masses, it can be modelled with n degrees of freedom in a linearized form in the following way:

$$[M]\underline{\ddot{x}} + [C]\underline{\dot{x}} + [K]\underline{x} = \underline{F}(t) \tag{3.1}$$

- $[M]$ is the mass matrix $N \times N$
- $[C]$ is the damping matrix $N \times N$
- $[K]$ is the stiffness matrix $N \times N$
- $\underline{\ddot{x}}$ is the acceleration vector
- $\underline{\dot{x}}$ is the velocity vector
- $\underline{x}$ is the displacement vector
- $\underline{F}(t)$ is the external force vector

If we know all the parameters of the system of these 3 matrices, we can simulate the behavior of the system in any condition. This approach is easy to understand and relatively easy to compute for low order systems, but as the degrees of liberty increases, computations becomes exponentially complex since the state of a single degree of freedom is dependent on the other states. To mitigate this issue, a commonly adopted method is **modal analysis**. This technique translates the position and movement of the n degrees of freedom into a function of the modes of vibration rather than the position of a point of mass. This approach, known as the **Modal Superposition Approach**, can be interpreted as the superposition of n single degrees of freedom that are independent of one another, this is a key concept. This innovative degree of freedom is termed **nodal modes**, illustrating how a structure or material vibrates in simple terms:

$$[\overline{M}]\underline{\ddot{x}} + [\overline{C}]\underline{\dot{x}} + [\overline{K}]\underline{x} = \overline{\underline{F}(t)} \tag{3.2}$$

1. $\overline{M}$ represents the mass matrix in its new representation as a function of modal nodes $N \times N$.
2. $\overline{C}$ represents the damping matrix in its new representation as a function of modal nodes $N \times N$.
3. $\overline{K}$ represents the stiffness matrix in its new representation as a function of modal nodes $N \times N$.

3.1.3. Modal approach and Frequency Response Function

When it comes to the steel strip, estimating the mass is straightforward, given the known material and dimensions of the strip. While stiffness and damping matrices can be computed using properties of the material and the geometry of the strip, this approach tends to be generalized.

Alternatively, utilizing data directly from the plant enables us to customize the model to the specific steel strip under consideration. However, for other parameters related to $\overline{C}$ and $\overline{K}$, experimental data is essential to complement the theoretical approach.

Since the modal approach allows us to consider each resonance frequency independently, we can use a superimposition approach. Consider the transfer function from a force applied to physical coordinate k to the displacement of physical coordinate j:

$$G_{jk}(i\omega) = \sum_{n=1}^{N} \frac{X_{0j}^{(i)} X_{0k}^{(i)}}{-\Omega^2 \overline{m}_{ii} + i\Omega \overline{c}_{ii} + \overline{k}_{ii}} \tag{3.3}$$

- $X_{0j}^{(i)}$ is the modal displacement of the j-th coordinate
- $X_{0k}^{(i)}$ is the modal displacement of the k-th coordinate
- $\overline{M}_{ii}$ is the modal mass of the i-th coordinate
- $\overline{C}_{ii}$ is the modal damping of the i-th coordinate
- $\overline{K}_{ii}$ is the modal stiffness of the i-th coordinate
- Ω is the discrete frequency considered

This explains how the resulting displacement on a specific K coordinate is the sum of all the modal displacements of resonance frequencies on coordinate K. From this equation, we can not only plot how the strip behaves at any frequency, but we would be able to identify the parameters for the modal matrices $\overline{C}$ and $\overline{K}$. Mechanical systems that vibrate theoretically possess infinite resonance frequencies and modes of vibration. The term "natural frequency" denotes a specific frequency at which the system naturally vibrates, while the concept of "mode" elucidates the particular manner in which the vibration occurs.

So now we are considering a system which explains a structure of a massive mass based not on the position of its point but on its resonance frequencies and its modal nodes. This way of reasoning can be applied to simple structures and through wave equations we can simulate the behavior of the structure.

3.1.4. Masses and Springs Model

An important simplification we make to achieve a working model is to assume **the steel strip to be static, instead of being dynamic and moving along the rollers**. We will now show how, though we have different modes of vibration, only one of them is relevant for our analysis. The strip is under tension and the rollers are bending the strip in different ways.

In the figure below, we show how the strip is being bent. Note the pass line is the equilibrium point of the strip. *Based on the following paper, The vibrations in hot dip continuous galvanization systems are of 3 different natures: [4]*

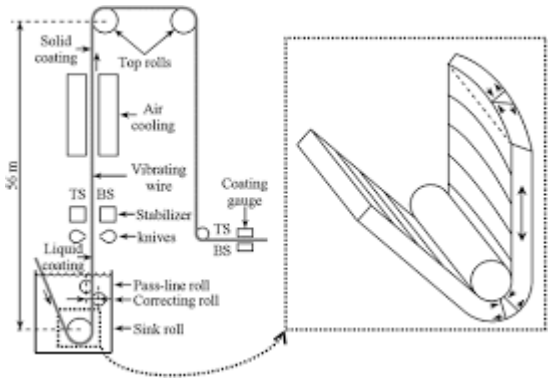

Figure 3.4: Coating segment bending

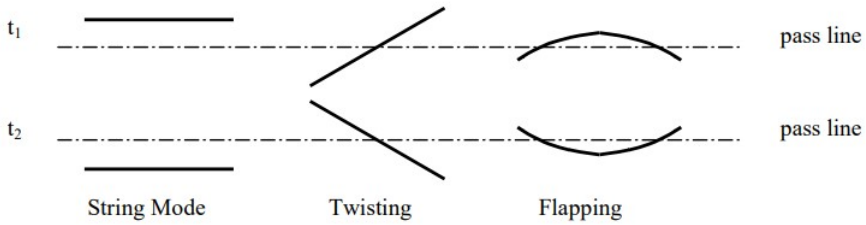

Figure 3.5: 3 different types of vibrations

1. **String Mode** This has more transversal movement, and it is the one we are more interested in
2. **Twisting** The extremes of the section are in counter-phase.
3. **Flapping** The extremes of the section are in phase.

Due to this consideration theoretically every steel strip owns three different kind of infinite resident frequencies and modes of vibration. The papers authors concluded that in the context of galvanization lines, the flapping effect is negligible, whereas the string mode and twisting are of paramount significance.

Consequently, in our current 1D model, we will only account for and explain the string mode. The twisting mode, on the other hand, necessitates a 2D model, which could provide a more accurate description of the system but demands increased complexity. It's important to note that the twisting mode corresponds to a distinct type of vibration occurring in a different dimension. In the final analysis, our primary focus lies on the string mode.

So, considering only a string as way of vibrating, a system in one dimension can be seen as a series of masses and springs connected together, tied together and linked to extremities

who are fixed. Utilizing classical definitions for both the mass and the stiffness:

$M_{tot} = \rho \cdot w \cdot h \cdot l$

$K_{tot} = \frac{\sigma \cdot w \cdot h \cdot}{l} + \frac{\sigma \cdot h^3 \cdot E}{12 \cdot l^3}$

- w is the width of the strip $[m]$
- h is the thickness of the strip $[m]$
- l is the length of the strip $[m]$
- E is the Young's modulus of the strip $[Pa]$
- ρ is the density of the strip $[kg/m3]$
- σ is the tension of the strip $[N]$

In this application, the steel strip is fixed in position from two rollers, one bottom roller immersed in the bath of zinc, and one top roller at 20 meters from the bottom roller. The steel strip stretches in length for 20 m, in width for 1 m and in thickness for 1.5 mm, making it a very thin and long structure. In essence, a complex geometrical shape exhibits various natural modes, representing different ways in which it can undergo bending. As we just saw, we will be considering only one. The stiffness parameter K_{tot} is the sum of the stiffness of the material, physical propriety, and the stiffness of the stress applied to the strip from both sides along it's length. The strip is under tension and the rollers are bending the strip.
Given that we are discussing thin strips or elements with a structure measuring just a few millimeters (1.5 mm), it becomes evident that the element related to the tensioned string is nearly negligible. This is because we are dealing with elements that are significantly wider in terms of length and width compared to their thickness.
As a result, we aren't committing a significant error by disregarding the second element of stiffness. This conclusion leads us to assert that, in terms of oscillations, a stretched tape behaves in practice much like a rope. Therefore, we can apply the same equations used for ropes to calculate resonance frequencies and the modes shapes.
Resonance frequencies of a rope:

$$f_n = \frac{n}{2l}\sqrt{\frac{\sigma}{\rho}} \tag{3.4}$$

Where n is the mode of vibration, l is the length of the rope, σ is the tension of the rope and ρ is the density of the rope. Thus we now have a theoretical model to determine the

resonance frequencies of the steel strip.

⊛*Mode*	**1**	**2**	**3**	**4**	**5**	**6**	**7**	**8**	**9**
Hz	0.05	0.1	0.15	0.20	0.25	0.30	0.35	0.40	0.45

3.2. Finite Element Method

Now that we can compute the resonance frequencies of the steel strip, let's determine a way to simulate the behavior of the strip.
Theoretically the masses are represented as points in the spatial representation, whereas we are considering an expanded and flat steel strip, a different and larger geometry. In this case the normal theoretical approach isn't feasible, since we are considering a complex geometry, and we need to represent it into matrices. Using the Finite Element Method we discretize the long steel strip into smaller elements to analyze their mechanical behavior. Imagine the steel strip as a continuous material, but for the sake of analysis, we divide it into smaller elements. These elements can be linear or curved, approximating the strip's geometry. The strip is essentially meshed, forming a finite number of elements. Next, we consider the behavior of each element using relevant equations and principles of material mechanics. The FEM employs mathematical modeling, often using equations derived from elasticity and stress-strain relationships, to simulate the deformation and stress distribution within each element. The key is to establish how these individual elements interact with each other at their boundaries, sharing forces, displacements, and stresses. This interaction is represented through a system of equations based on the physical properties of the material and the element's geometry, which will be represented via the mass, spring and damper matrices mentioned above: $\overline{M}$, $\overline{K}$ and $\overline{C}$ By solving these equations for the entire mesh of elements, we obtain a comprehensive understanding of how the steel strip responds to various set of external loads, boundary conditions, and constraints.

When examining the steel strip along its length, even though we are dealing with a segment that could be as long as 20 meters or more, with a thickness of 1.5 mm and a width of 1 meter, we can simplify this segment as a beam. A beam is a structure longer in one direction and shorter in the other two compared to the first. Consequently, we are compressing the structure into one dimension, which is the length of the beam.

We are splitting the beam into smaller elements, which are the Finite Elements, with the aim of simulating the behavior of the entire beam, once the resonance frequencies of beam are known.

An important assumption for FEM materials would be to have each finite element single stand-alone system to have its own natural frequencies higher than the maximum forcing effect frequency Ω_{max} applied on any point of the system

$$\Omega_{max} \ll \omega_{k1} \tag{3.5}$$

being ω_{k1} the lowest natural frequency of the system of the k-th FE element.

We know that boundary conditions affect the natural frequencies of the system, but won't change their magnitude of the vibrations, we can consider that:

$$\omega_{k1} = \frac{\pi}{L}^2 \sqrt{\frac{EI_k}{m_k}} \lll \Omega_{max} \tag{3.6}$$

This leads us to conclude the maximum length of the beam of the FEM element should be:

$$L_k \lll L_{k,max} = \frac{\pi}{\sqrt{c_s \Omega_{max}}} \sqrt[4]{\frac{EI_z}{m}} \tag{3.7}$$

Where Ω_{max} is the maximum frequency of the excitation disturbance, E is the young modulus of the material and I_z is the moment of inertia around the length axis, and m the mass.
This limits the length of the FEM beam element, and we will need to consider a higher number of elements to represent the entire length of the steel strip.

$$L_{k,max} = \frac{\pi}{\sqrt{c_s \Omega_{max}}} \sqrt[4]{\frac{EI_z}{m}} = 1.57 meters \tag{3.8}$$

- Ω_{max} is the maximum frequency of the excitation disturbance $= 15[Hz]$
- E is the young modulus of the material $= 2.1e11[Pa]$
- I_z is the moment of inertia around the width axis $1.3021e-08[m^4]$
- C_s is the "safety coefficient" $= 2$
- m the linear mass $= 48.7500[Kg/m] = [\rho \cdot m^2]$

The theoretical maximum length of the beam element is 1.57 meters, but we will consider a length of 1 meter for the beam element.

3.2.1. Finite Element matrices

Let's establish the Finite Element matrices for the simulation. While we can theoretically compute a Frequency Response Function (FRF) for any force and any point in the system, the Finite Element Method enables the derivation of a more personalized FRF from any point to any point. If we had a system with 20 degrees of freedom, we would need to determine the mechanical equations for each degree of freedom. Additionally, we can simulate the transformation of the system in the time domain, extending this approach to a velocity and acceleration domain.

The steel strip will be simulated as a series of masses, springs and dampers connected together. We are taking into consideration a sheet long 20 meters, and we are dividing it into 20 elements, each element is 1 meter long Thickness and width are considered in the mass constant $\widetilde{m}$.

For each of the 20 elements, we will consider 3 degrees of freedom:

- Axial displacement u_i
- Transverse displacement v_i
- Rotation θ_i

Leading us to have 6x6 matrices for each element, and a total of 120x120 matrices for the entire system. This is a very large system, but the length of the beam is within the maximum length admitted from the FEM assumption we mentioned earlier. Mass matrix for the local element

$$mL = \widetilde{m} \cdot l \begin{bmatrix} \frac{1}{3} & 0 & 0 & \frac{1}{6} & 0 & 0 \\ 0 & \frac{13}{35} & \frac{11l}{210} & 0 & \frac{9}{70} & -\frac{13l}{420} \\ 0 & \frac{11l}{210} & \frac{l^2}{105} & 0 & \frac{13l}{420} & -\frac{l^2}{140} \\ \frac{1}{6} & 0 & 0 & \frac{1}{3} & 0 & 0 \\ 0 & \frac{9}{70} & \frac{13l}{420} & 0 & \frac{13}{35} & -\frac{11l}{210} \\ 0 & -\frac{13l}{420} & -\frac{l^2}{140} & 0 & -\frac{11l}{210} & \frac{l^2}{105} \end{bmatrix} \tag{3.9}$$

Stiffness matrix for the local element

$$kL_{ax} = \frac{EA}{l} \begin{bmatrix} 1 & 0 & 0 & -1 & 0 & 0 \\ 0 & 0 & 0 & 0 & 0 & 0 \\ 0 & 0 & 0 & 0 & 0 & 0 \\ -1 & 0 & 0 & 1 & 0 & 0 \\ 0 & 0 & 0 & 0 & 0 & 0 \\ 0 & 0 & 0 & 0 & 0 & 0 \end{bmatrix} \tag{3.10}$$

Contribution of the longitudinal deflection

$$kL_{fl} = EJ \begin{bmatrix} 0 & 0 & 0 & 0 & 0 & 0 \\ 0 & \frac{12}{l^3} & \frac{6}{l^2} & 0 & -\frac{12}{l^3} & \frac{6}{l^2} \\ 0 & \frac{6}{l^2} & \frac{4}{l} & 0 & -\frac{6}{l^2} & \frac{2}{l} \\ 0 & 0 & 0 & 0 & 0 & 0 \\ 0 & -\frac{12}{l^3} & -\frac{6}{l^2} & 0 & \frac{12}{l^3} & -\frac{6}{l^2} \\ 0 & \frac{6}{l^2} & \frac{2}{l} & 0 & -\frac{6}{l^2} & \frac{4}{l} \end{bmatrix} \tag{3.11}$$

Contribution of the axial deflection due to the tension force

$$kL_P = P \cdot \frac{l^2}{30} \begin{bmatrix} 0 & 0 & 0 & 0 & 0 & 0 \\ 0 & \frac{36}{l^3} & \frac{3}{l^2} & 0 & -\frac{36}{l^3} & \frac{3}{l^2} \\ 0 & \frac{3}{l^2} & \frac{4}{l} & 0 & -\frac{3}{l^2} & -\frac{1}{l} \\ 0 & 0 & 0 & 0 & 0 & 0 \\ 0 & -\frac{36}{l^3} & -\frac{3}{l^2} & 0 & \frac{36}{l^3} & -\frac{3}{l^2} \\ 0 & \frac{3}{l^2} & -\frac{1}{l} & 0 & -\frac{3}{l^2} & \frac{4}{l} \end{bmatrix} \tag{3.12}$$

Assmebly of the global stiffness matrix

$$kL = kL_{ax} + kL_{fl} + kL_P \tag{3.13}$$

For the damping matrix, we will consider a damping ratio of 0.001, which is a very small damping ratio, but it provides a reasonable approximation for the steel strip. For this first approach, we considered such a low damping ratio since metallic ma we used a heuristic approach to identify the damping matrix, but we will later on use a more accurate approach to identify the damping matrix.

4 | Steel Strip Modes

4.1. Identification of a Steel Strip Modal nodes

The data raw data coming from the sensors is not usable, it needs to be preprocessed and cleaned. The software IBAAnalyzer is used to clean the data and obtain a more usable format. The data is then processed in Matlab to obtain the Frequency Response Function (FRF) of the steel strip. In this segment is to identify the modal shapes and frequencies of a steel strip, via measurements coming from the sensors of the line.
Let's first describe the actuators and sensors involved in out system:

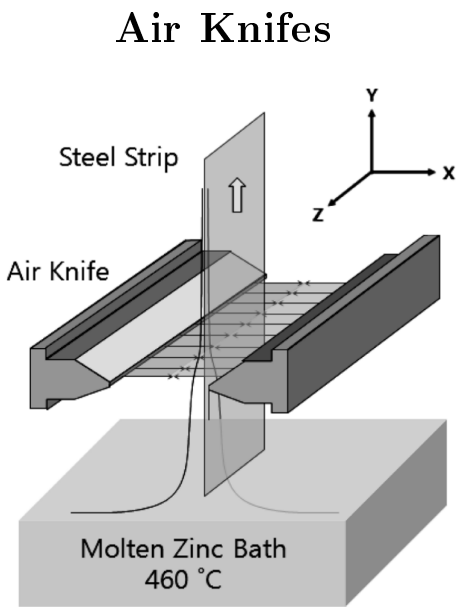

Figure 4.1: Air Knifes

The actuator are the air knifes which apply pressurized air along a thin and wide area on the steel strip to both remove from the steel strip the excess of zinc and to cool down the steel strip, after being immersed in a 450° C zinc bath. They act on both sides never together, but always in an alternate way. In our control system, these air streams function

as disturbances to the steel strip unpredictably. As their switching law is unknown, and their magnitude is not constant, we will utilize white noise to simulate their effect on the steel strip. The maximum amplitude of the white noise is set at 100 N.

Inductive Sensors

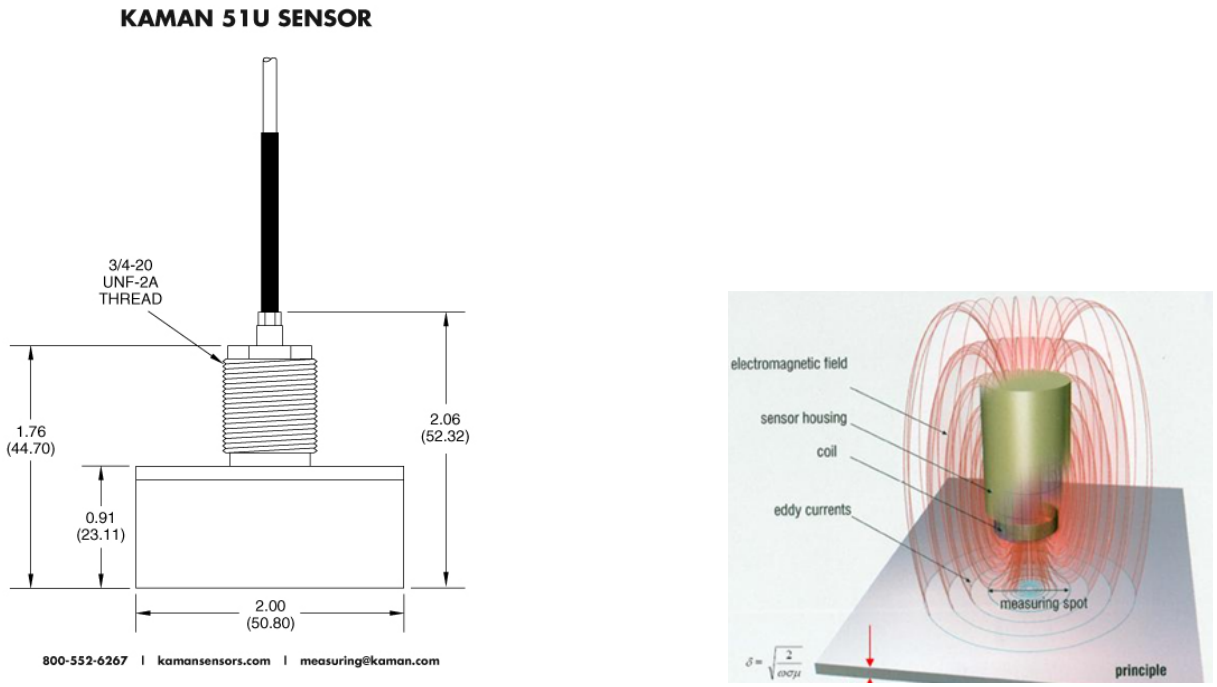

Figure 4.2: Magnetic Stabilizer dimensions (left) and Magnetic Field Generated (right)

Across the width of the air knives there are 8 of these sensors on both sides, for a total of 16, which measure their distance from the steel strip. They have a standard range of 25 mm, with a static resolution of 0.01 mm, so they are able to work reliably with a high precision. They sense the variation of the magnetic field they generate caused by the presence of the steel strip. Though these sensors work using magnetic fields, thus applying a force on the ferrous strip, the magnitude of such attractive force is trivial compared to the actuators and other forces in play.

4.1.1. Vibrational Analysis

We need to identify experimentally the natural frequencies of the steel strip. We could obtain them by using theoretical result by applying vibrational theory using the strip proprieties, but reality usually never matches the theory. To have a more concrete and practical approach we will be using data.

Through ammeter we can measure the current applied to the magnetic stabilizers. The

values have been collected via several experiments.
The data collected is available in the following table:

- **time**: in seconds
- **current**: in Ampere applied to electromagnet i-th on the front. $\sum_{i=1}^{8} current_i = currentappliedtoelectromagneti-th$
- **current_back**: in Ampere applied to electromagnet j-th on the back. $\sum_{j=1}^{8} current_i = currentappliedtoelectromagnetj-th$
- **position**: in mm of the steel strip from the front. $\sum_{i=1}^{8} position_i = positionofthesteelstripfro$
- **position_back**: in mm of the steel strip from the back. $\sum_{j=1}^{8} position_i = positionofthesteelst$

The data collected has been processed in order to obtain a simple format, coming from both sides. It has been seen that the data coming from the front and back are very similar, only reversed. This corroborates the accuracy of the data collected.
We can use data given by the induction sensors to perform a vibration analysis of the steel strip. **Vibration analysis** is a technique used by analyzing signals which can have two different goals:

1. **Signal Analysis**: to assess the nature and origin of vibrations
2. **System Analysis**: in order to derive a mathematical model of the system

In our case, our primary interest lies in the system analysis. We can acquire signals from the sensors during both operational and non-operational conditions. Operational conditions refer to when the plant is actively running, while non-operational conditions pertain to periods when the plant is not functioning. From a theoretical standpoint, it is more prudent to collect data during non-operational conditions since the system is not in operation and is not subjected to external stimuli.
Due to the nature of the system in study, only during operating conditions data was available. Any still time in the galvanization leads to thousands of lost profit and additional cost, so they are rare.

4.1.2. Frequency Response Function

To extrapolate the desired resonance frequencies of the strip in order to obtain experimental natural frequencies, we will be using the Frequency Response Function (FRF). It's a function which describes the output spectrum of a system relative to a given input

spectrum. In our case, the output signal is the position detected by the induction position sensor, while the input signal is explained in the following paragraph.

The input signal is derived by the electromagnetic stabilizer, a complex and refined system of electromagnets. These electromagnets working some in AC and some in DC, the reason has already been explained. There is a set working in AC on both sides of the strip. Then each is positioned between different 2 sets of electromagnets working in DC, for a final count of 6. Each set is composed of 8 electromagnets who are able to generate an attractive magnetic force, pulling the steel strip towards them, working independently of one another. The hold the following structure:

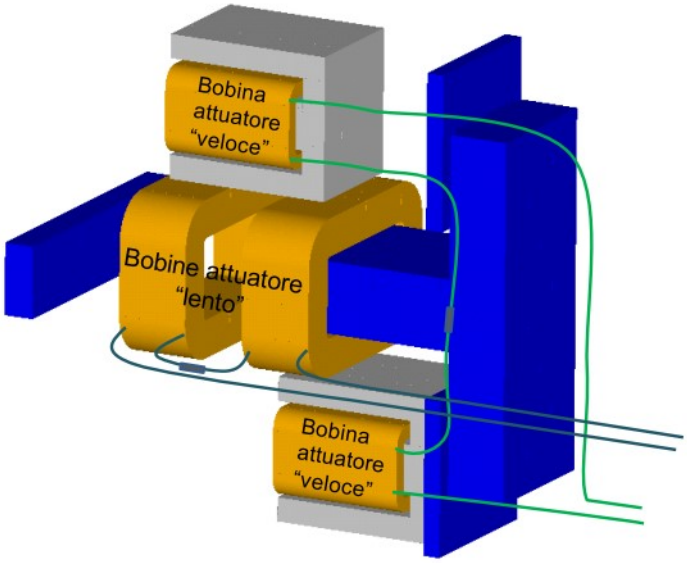

Figure 4.3: Slow actuators (DC) and fast actuators (AC)

By working in synchronization the electromagnets from both sides can ideally maintain the steel strip in a stable position, pulling it towards them, like a never ending tug of war. An ideal conclusion would be to find the current required to generate a certain force to, as if we were looking for a proportional relationship, but this is a monumental task to undertake. As mentioned in the following article,

"the attractive force generated by the electromagnets it is a non-linear function which is a function of the current applied to the electromagnet and the distance of the steel strip from the electromagnets. The following plot from a paper describes better the following concept":[5]

To add motives to this simplification and address this challenge, **we will use the force applied to the strip as the input signal for our Frequency Response Func-**

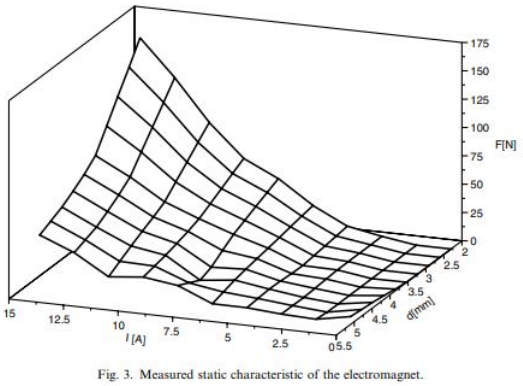

Figure 4.4: *Force generated by the electromagnets[5]*

tion, rather than the current. This decision can be further justified by the following considerations:

1. We can create a high-frequency (hundreds of hertz) control loop for the current. In this context, any changes in voltage V or current i can be viewed as a rapidly varying disturbance, which any controller can effectively reject. From a mechanical system perspective, the current loop operates so swiftly that we can assume current changes occur instantaneously.

2. The potential transfer function between the input current and the output applied force exhibits a very low time constant and a high bandwidth. As a result, it changes rapidly, and its magnitude has minimal impact on the overall outcome. It can effectively be considered a unitary gain. In contrast, the mechanical response of the strip has a higher time constant and a lower bandwidth, causing it to change more slowly.

3. The frequencies of interest are in the range of 1 to 100 Hz. The current loop operates at a much higher frequency, and reaches steady state conditions way faster.

Air Knifes

A basic FRF can be obtained by using the following formula:

$$H(\omega) = \frac{output}{input} = \frac{movement}{force} = \frac{response}{excitation} \tag{4.1}$$

The FRF has 3 different basis: displacement, velocity and acceleration. A more precise definition of the FRF is the following:

$$\alpha_{jk} = \frac{x_j}{F_k} = \sum_{nr=1}^{N} \frac{\Phi_j^r \Phi_{jk}^r}{\lambda_r^2 - \omega^2} \tag{4.2}$$

- α_{jk} is the receptance matrix
- λ_r is the eigenvalue of the r^{th} mode (modal frequency + modal damping)
- Φ_j^r the j^{th} component of the r^{th} natural shape vector (modal shape). i.e: $\{\Phi\}$ relative displacement at the j^th degree of freedom of the r^th shape
- N is the number of modes considered

There are several testing configurations available which can be compared: SISO, SIMO, MISO, MIMO.

1. SISO: Single Input Single Output
2. SIMO: Single Input Multiple Output
3. MISO: Multiple Input Single Output
4. MIMO: Multiple Input Multiple Output

The signal is measured in time domain, but it is analyzed frequency domain using the FFT (Fast Fourier Transform) algorithm. If we have a SISO representation, we can use the following formula to obtain the FRF:

$$X_p = \frac{H_{pq}}{F_q} \tag{4.3}$$

or in a MIMO representation:

$$\begin{bmatrix} X_1 \\ X_2 \\ .. \\ .. \\ X_n \end{bmatrix}_p = \begin{bmatrix} H_{11} & H_{12} & .. & .. & H_{1n} \\ H_{21} & H_{22} & .. & .. & H_{2n} \\ .. & .. & .. & .. & .. \\ .. & .. & .. & .. & .. \\ H_{n1} & H_{n2} & .. & .. & H_{nn} \end{bmatrix} \begin{bmatrix} F_1 \\ F_2 \\ .. \\ .. \\ F_n \end{bmatrix}$$

Where X represents the position of the steel strip, H represents the FRF and F represents the force applied by the magnetic stabilizers. As an example, of the applied force of application, we can show the following:

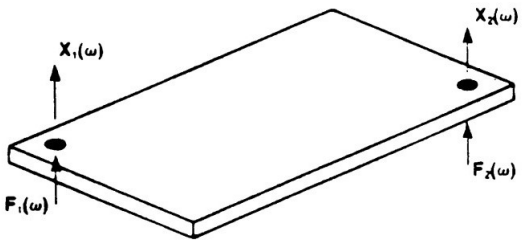

Figure 4.5: FRF Theoretical

We can apply an excitation to the strip in different positions, but in case of the current steel strip, sensor position and excitation position are fixed on the same distance, with respect to the length of the steel strip.
Sensors and actuators are looked on certain coordinates along the length of the steel strip, respectively:

- Sensors: 17 m
- Actuators (Electromagnets): 17.5 m
- Air knifes (Disturbance): 18.5 m

In our case we had a MIMO (multiple input multiple output) where the inputs are the magnetic stabilizers and the outputs are the induction sensors From both sides.

For further research, a 2D model can be developed, which takes into consideration the twisting of the steel strip. This can be more accurate, but it is also more complex and requires further studying. The amount of data available makes it a feasible line of research.

4.1.3. Excitation

Now we have explained why we are using a 1 dimensional approach, we can explain how we are going to excite the system.
For vibration analysis, various excitation signals can be used, each one with its own advantages and disadvantages.

- excitation by means of dynamic exciter
  - by harmonic signal
  - by random signal
  - by other types of signals
- impulse excitation
  - by means of impact hammer
  - step release (from deformed position)

The excitation signal applied was a multi-sine signal, with spanning frequencies from 1 to 100 Hz. Its notable advantage lies in its ability to cover the entire frequency spectrum of the mechanical system under study within a brief duration, effectively exciting all the modal frequencies. This short testing window enables experiments to be conducted within an industrial environment during periods of downtime. In the galvanization industry, even a few minutes of downtime can result in substantial financial losses with no corresponding benefits.
The excitation signal was applied to the magnetic stabilizer, using the following formula:

$$u(t) = \sum_{k=1}^{N} A_k sin(\omega_k t + \phi_k)$$

where: A_k is the amplitude of the signal, ω_k and ϕ is the phase of the signal. In a moment where the plant was not in motion, with no disturbance from the air knifes, this signal was applied to the magnetic stabilizers. The signal was applied in a single manner, meaning that the signal was applied to all the magnetic stabilizers at the same time. By reading the FRF response to an excitation signal, and then observing the peaks of the FRF, we can identify the resonance frequencies of the steel strip.

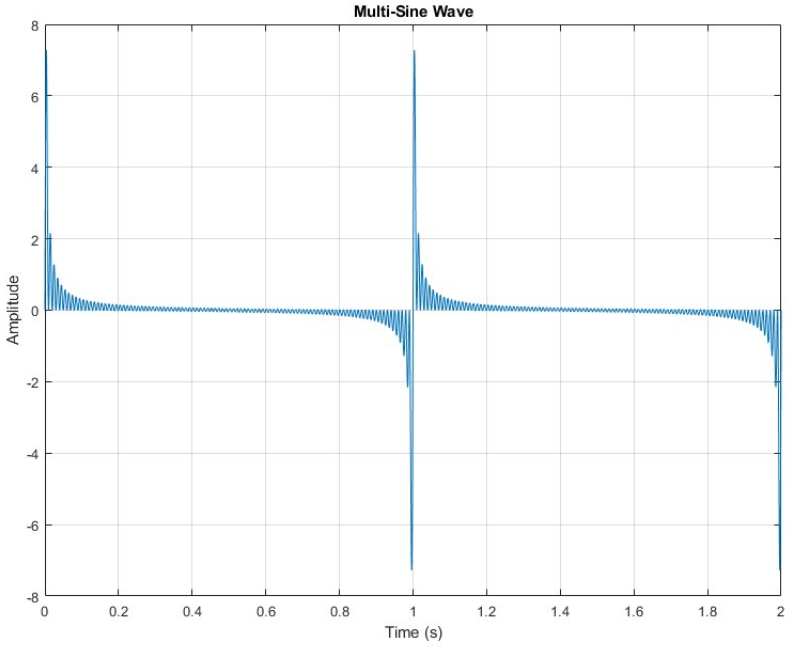

Figure 4.6: Multi-sine signal

5 | Frequency Response and Finite Element Method

5.1. Identification of Modal Parameters

Given our utilization of the Frequency Response Function (FRF), the system is presumed to be linear and time-invariant. Even though we applied a multi-sine excitation, our focus will be on the portion of the dataset where the system is free from external excitation, specifically the concluding section. This choice is influenced by the realization that the system didn't have sufficient time during the experiment to reach an unexcited state, a prerequisite for accurately detecting the natural frequencies.

For this reason, we will exclusively analyze the latter part of the dataset where the system is devoid of external excitation. In this context, the final segment of the multi-sine excitation can be treated akin to an impulse response. This impulse response concept is analogous to using an instrumental hammer, and, as such, the concluding segment of the dataset will be regarded as an impulse response.

So after the impulse response we are observing a free damped motion.

Using both an impulse and multi-sine excitation, we apply an H1 algorithm to obtain an experimental FRF:

The peaks observed in the frequency domain from the multi-sine excitation are not as distinct as those obtained from the impulse response. They appear closely spaced and lack well-defined characteristics.

Contrastingly, the peaks derived from the impulse response are clear and exhibit a closer resemblance to the theoretical results. Consequently, the peaks identified through the impulse response will be the focus of our analysis.

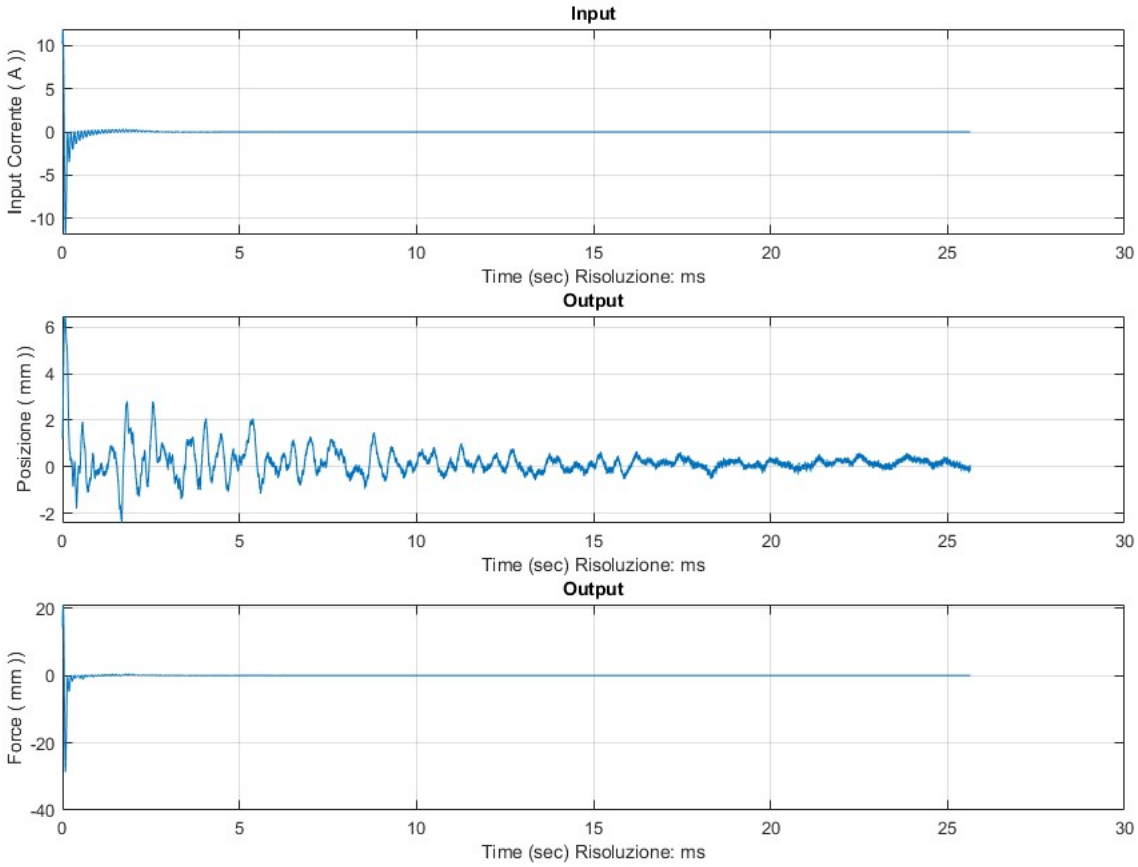

Figure 5.1: Impulse Response in Time Domain

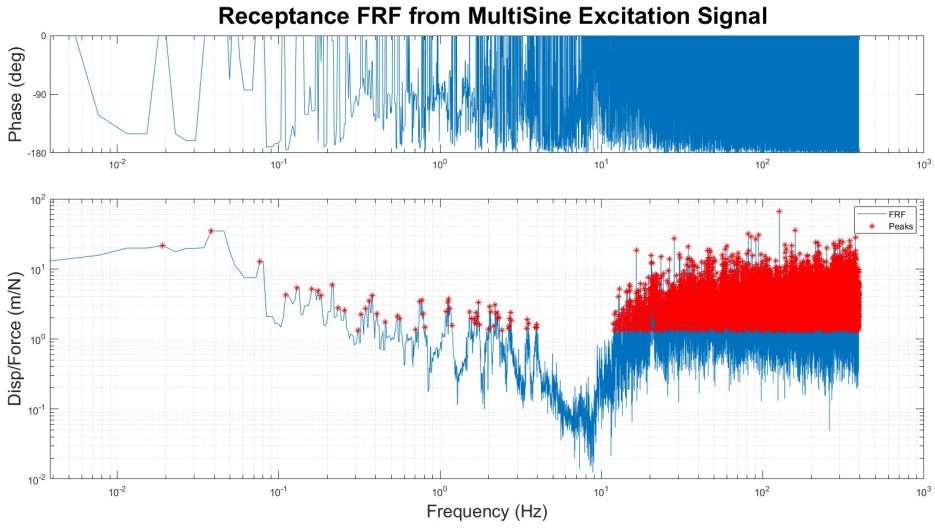

Figure 5.2: Receptance FRF obtained using multi-sine excitation

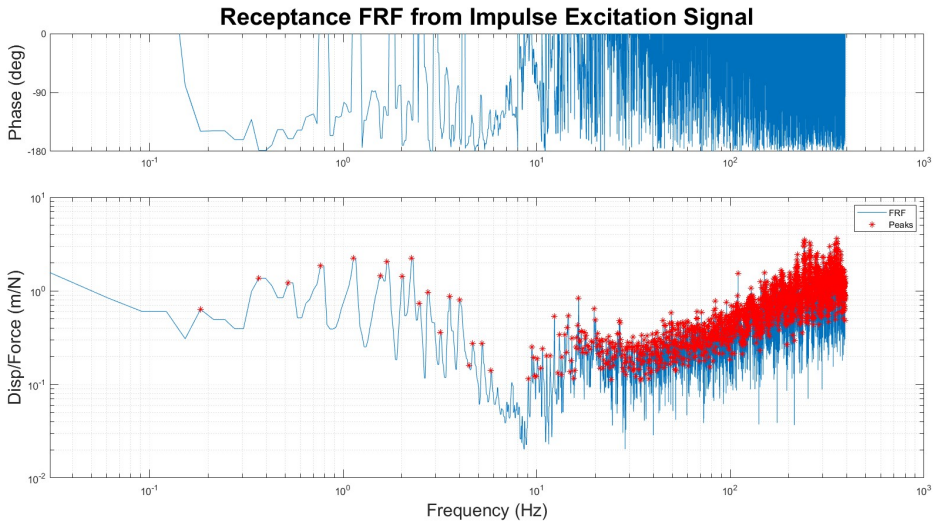

Figure 5.3: Receptance FRF obtained using impulse response. $*$ corresponds to the peaks identified

5.1.1. Comparison

Comparing the theoretical modes of vibration to the modes of vibration obtained with real data from the frequency response functions:

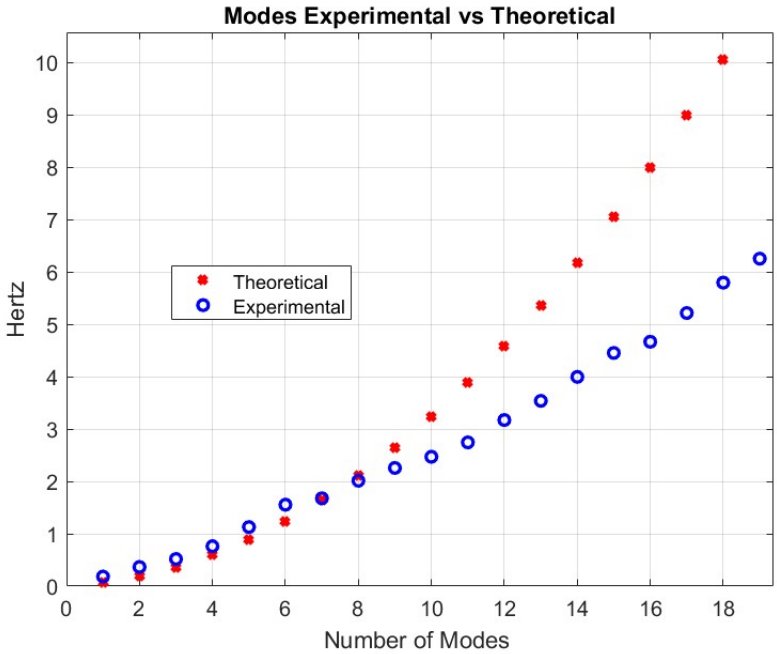

Figure 5.4: Theoretical vs Experimental modes of vibration of a steel strip

We can notice that the theoretical and experimental modes of vibration are very similar,

but not identical. This is due to the fact that the theoretical model is a simplification of the real system, and that the real system is not a perfect system. This is very good the since we are interested only in the first modes of vibration, since they are the most energy dense and powerful. Generally, the higher (in order) is the frequency, the larger is the difference between theoretical (computed) and measured values. We observe that beyond the 10th mode, the disparity between theoretical and experimental results becomes increasingly pronounced, indicating that the theoretical model is no longer a robust approximation of the real system. Therefore, let's explore using only the first 10 modes of vibration to simulate the system.

The table below are the resonant frequencies of the system, identified from the FRF theoretically and experimentally using the data provided by the multi-sine excitation, or specifically the impulse response of the system.

Table 5.1: Experimental and Theoretical Vectors

Index	Experimental	Theoretical
1	0.1831	0.0670
2	0.3662	0.1840
3	0.5188	0.3600
4	0.7630	0.5950
5	1.1292	0.8880
6	1.5564	1.2400
7	1.6785	1.6510
8	2.0142	2.1210
9	2.2584	2.6490
10	2.4720	3.2370
11	2.7467	3.8830
12	3.1739	4.5880
13	3.5401	5.3520

To make comparison between modes is often done by a simple tabelation of both result sets, but a more useful form is to draw the experimental value and the theoretical value. This is done to see if and up to which natural frequencies the theoretical model is a good approximation of the real system.

In the graph we can see that the theoretical and experimental modes of vibration are very similar, but not identical. The differences should have the tendency that the theoretical values of frequencies are higher than the measured ones, because usually damping is not included in the theoretical values whereas measured frequencies are always damped and thus of lower values. Realize that the more modes of vibration we consider, the more complex the system becomes, and the more difficult would become our system.

It is necessary to choose those points from the theoretical model (which usually has much more degrees-of-freedom than experimental model) that coincide with the experimental model.

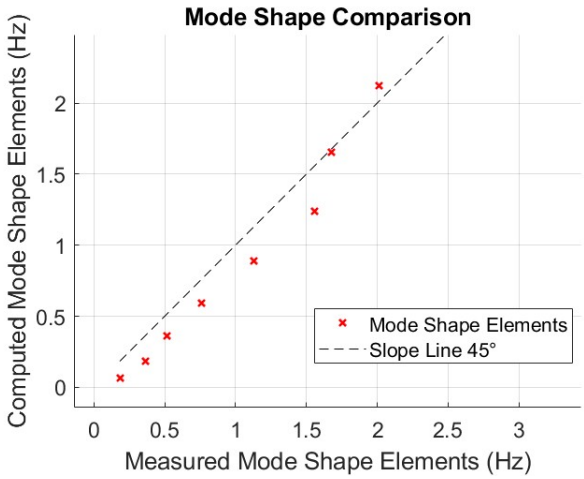

Figure 5.5: 4 modes of vibration of a steel strip

In this way, not only the degree of consistency between the two sets of results can be seen, but also the nature and possible causes of the discrepancies.

The drawn points should lie on the line with the slope 1 or near this line. If they lie near a line with the slope other than of 45°, the cause of this discrepancy is quite sure in incorrect material properties used for computation. Further on for out control scheme we will consider only the first 4 modes of vibration, for the sake of simplicity.

5.1.2. State Space Representation

In order to simulate the system, we can represent the system in state space form. The total displacement of the system can be written as a linear combination of each of the modal coordinates, which are function of the mass, stiffness and damping of the system, for each mode of vibration. The state space guarantees the independence of each mode of vibration, and the linearity of the system.

$$\begin{bmatrix} x_1 \\ \dot{x_1} \\ x_1 \\ \dot{x_2} \\ .. \\ .. \\ x_n \\ \dot{x_n} \end{bmatrix} = \begin{bmatrix} 0 & 1 & 0 & 0 & .. & .. & 0 & 0 \\ -\omega_1^2 & -2\zeta_1\omega_1 & 0 & 0 & .. & .. & 0 & 0 \\ 0 & 0 & 0 & 1 & .. & .. & 0 & 0 \\ 0 & 0 & -\omega_2^2 & -2\zeta_2\omega_2 & .. & .. & 0 & 0 \\ .. & .. & .. & .. & .. & .. & .. & .. \\ .. & .. & .. & .. & .. & .. & .. & .. \\ 0 & 0 & 0 & 0 & .. & .. & 0 & 1 \\ 0 & 0 & 0 & 0 & .. & .. & -\omega_n^2 & -2\zeta_n\omega_n \end{bmatrix} \begin{bmatrix} x_2 \\ F_1 \\ x_2 \\ F_2 \\ .. \\ .. \\ x_n \\ F_n \end{bmatrix}_p \tag{5.1}$$

- X_i is the modal coordinate of the i-th mode of vibration
- ω_i is the natural frequency of the i-th mode of vibration
- ζ_i is the damping ratio of the i-th mode of vibration
- F_i is the force acting on the i-th mode of vibration

6 | Control Scheme

6.1. Control Scheme

This section is dedicated in explaining the control scheme used to control the steel strip in simulation. As explained before, we are expressing the moving steel strip as a one dimensional system with fixed ends. We have computed the two following transfer functions from the Finite Element Model:

- **sys3638**: this transfer function describes the relation between the input force from the magnetic stabilizer to the output position of the steel strip.
- **sys3538**: this transfer function describes the relation between the input force from the air knife to the output position of the steel strip.

The first one can be considered as our main actuator, while the second can be considered as our known disturbance. Remembering, we are aiming to attenuate unknown external impulses, which act mostly on resonance frequencies of the structure itself. If we applied a white noise as an input to the transfer function associated to the air knife we are simulating how the steel strip would react to an external impulse when the air knife is active up to a magnitude of 100 Netwon.
As described by this following paper[1], we can use the pole placement method to place the poles of the system in a way that we can achieve the desired response. Out main goal is attenuate the magnitude in the resonance frequencies, without changing the modes. This can be achieved by **modifying the damping ratios of the natural frequencies**.
These can be explained by the following equation:

$$\mathcal{X}_A(s) = \prod_{i=1}^{m}(s^2 + 2\zeta_i\omega_{ni}s + \omega_{ni}^2) \tag{6.1}$$

By applying the pole placement controller such as:

$$L(s) = -\mathbf{K}(s\mathbf{I} - \mathbf{A})^{-1}\mathbf{B} \tag{6.2}$$

our intention is to obtain the following dynamics:

$$\mathcal{X}_A(s) = \prod_{i=1}^{m}(s^2 + 2\zeta_i^{\circ}\omega_{ni}s + \omega_{ni}^2) \tag{6.3}$$

$$L(s) = \frac{\prod_{i=1}^{m}(s^2 + 2\zeta_i^{\circ}\omega_{ni}s + \omega_{ni}^2)}{\prod_{i=1}^{m}(s^2 + 2\zeta_i\omega_{ni}s + \omega_{ni}^2)} - 1 = \frac{\beta(s)}{\prod_{i=1}^{m}(s^2 + 2\zeta_i\omega_{ni}s + \omega_{ni}^2)} \tag{6.4}$$

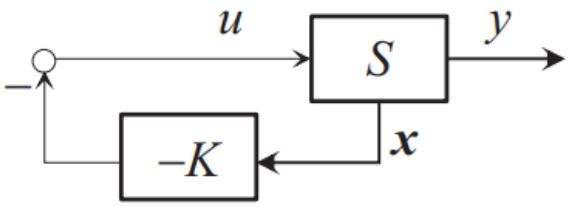

Figure 6.1: Block Diagram of the system

$$\beta(s) = \prod_{i=1}^{m}(s^2 + 2\zeta_i^{\circ}\omega_{ni}s + \omega_{ni}^2) - \prod_{i=1}^{m}(s^2 + 2\zeta_i\omega_{ni}s + \omega_{ni}^2) \tag{6.5}$$

$$\beta(s) = \prod_{i=1}^{m}(s^2 + 2(\zeta_i^{\circ} - \zeta_i)\omega_{ni}^{\circ}s + \omega_{ni}^2) \tag{6.6}$$

I have to show the difference between the two transfer functions, the one with the pole placement and the one without.

The Control Scheme

The sum of the transfer functions $sys3638$ and $sys3538$ can be seen as the final longitudinal position of the steel strip. Some further considerations are needed:

- **Measurement noise**: The inductive sensors employed for measuring the position of the steel strip are inherently susceptible to noise, though are very accurate.
- **Incomplete measurability of the system state**: We rely on the positions of various resonance frequencies as state space variables, rather than directly measuring the position of the system itself. Consequently, an observer is necessary to generate a state space estimation of the state variables, since each resonance frequencies is not objectively observable.
- **Incomplete controllability of the system**: While we employ a magnetic sta-

bilizer to control the system, we cannot exert control over the system across all frequencies, only the resonance frequencies.

- **Introduction of disturbance**: A disturbance is intentionally introduced into the system to account for additional external disturbances of unknown origin.

In case of the unmeasurable state variable, an observer is possible as mentioned by the paper, as well as the state system associated to the modes being observable.

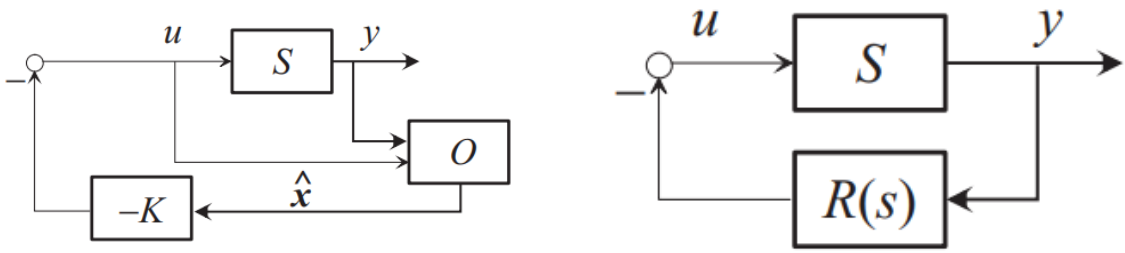

Output feedback with Observer (left) and Closed Loop System (b)

The resulting closed loop system is given is:

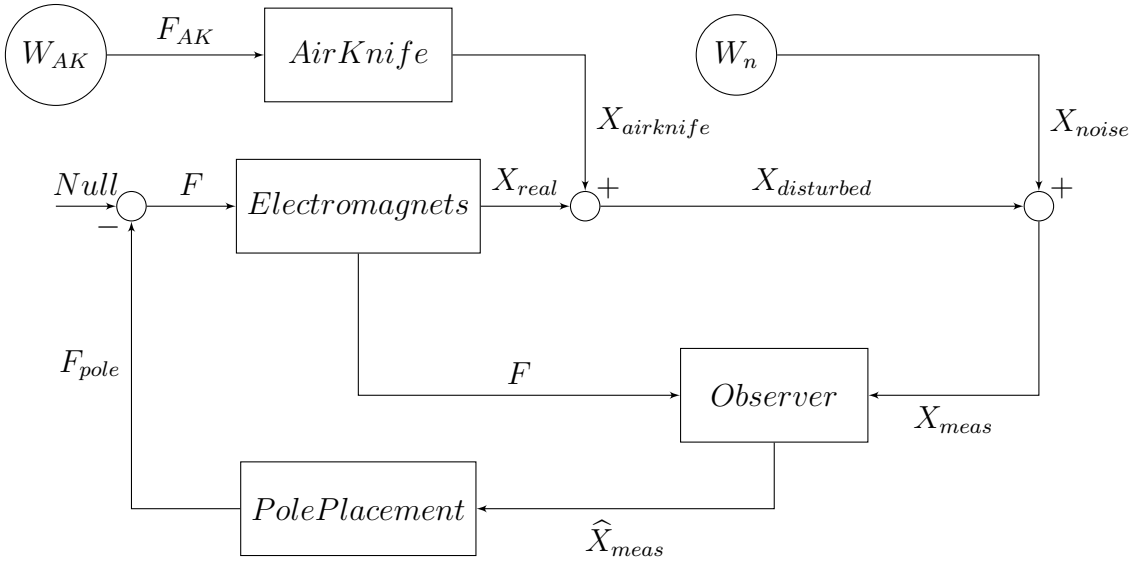

- X_{real}: real position of the steel strip, sum of all the modal shapes displacements
- F: force applied by the magnetic stabilizer in order to control the steel strip in position, equivalent to the control signal
- F_{AK}: force applied by the air knife in order to remove the excess zinc
- $X_{airknife}$: position of the steel strip caused by the disturbance of the air knife

- $X_{disturbed}$: position of the steel strip after the disturbance of the air knife
- X_{meas}: position of the steel strip after the measurement noise
- X_{noise}: white noise added to the system to simulate the measurement noise of the sensors
- $\widehat{X}_{meas}$: estimated position of the steel strip after the measurement noise on the Kalman Observer

6.1.1. Control Scheme

The following plots will have on the y-axis the displacement of the steel strip and on the x-axis the time. The show that our system works, we will apply via the air knifes a disturbance to the system.

We will be summing the two transfer functions $sys3638$ and $sys3538$ to simulate the real position of the steel strip, which will give us the final position of the steel strip, possibly close to the equilibrium set at 0.
At time output, we will be adding the white noise related to the Measurement noise of the inductive sensors. Though they are precise, we require to add some noise to simulate the real world.
Since the position of the resonance frequencies are not measurable, an observer is required. A Luenberger observer was insufficient in predicting the state variables accurately, so we used a Kalman Filter Observer. The Kalman Observer is able to predict to the position of the longitudinal position of the steel strip based on the previous state and the current state. This is possible since the Kalman integrates in the model an uncertainty matrix, which is able to predict the state of the system based on the previous state and the current state, while the Luenberger observer does not handle measurement noise as efficiently.
The following system is being disturbed by the air knife. The air knife is a system which uses a switching signal to stream air on one side only at the time. To simulate this, a white noise is used. The result is the following:

The observer is able to follow the phase, but the magnitude is not the same, since there is the added disturbance of the air knife and the measurement noise.

6.1.2. Result in the Pole Placement technique

To show the result of the pole placement technique, we will show the following plots to compare the system in open Loop without the controller and in closed loop.

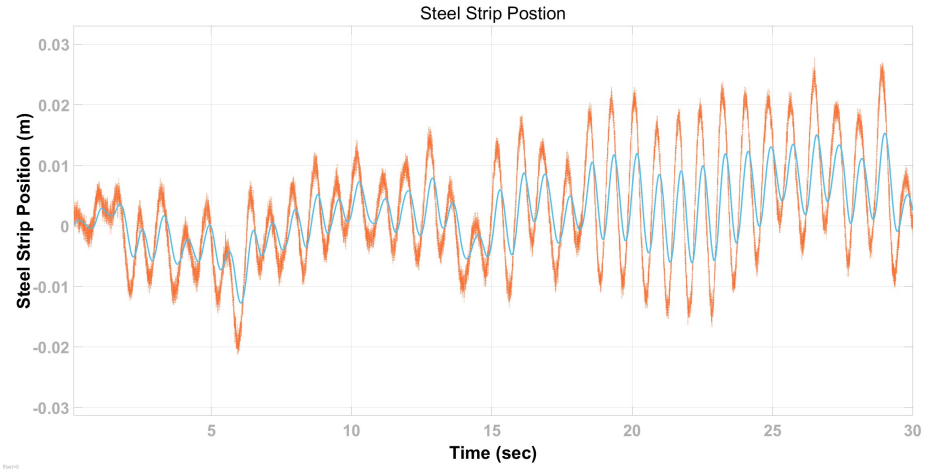

Figure 6.2: Observer result - Real position of the steel strip | Estimated position of the steel strip for Kalman Observer

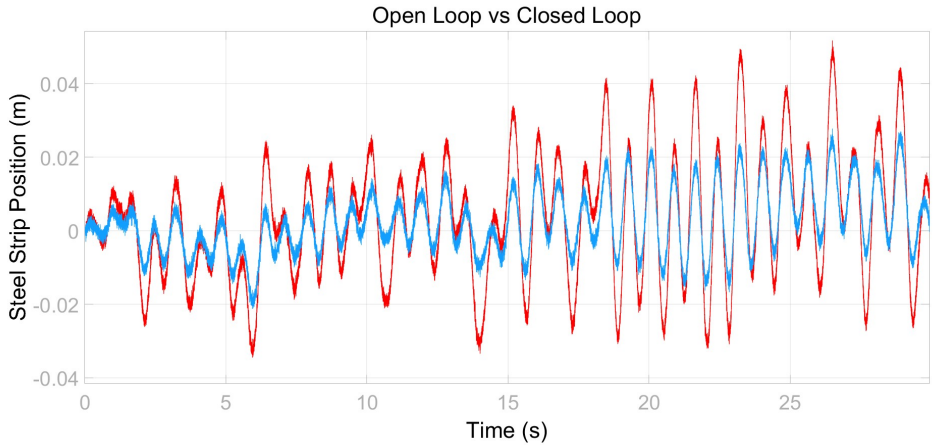

Figure 6.3: Open Loop | Closed Loop

The difference may not sound so big, but a critical safety condition for the steel strip would be to not exceed a certain threshold, which can be as tight as 2 cm. The efficacy of the system is contingent on the accuracy with which the observer can predict the position of the steel strip, taking into account the impact of noise.

6.1.3. Sensitivity Function

To show how this system is isolated from other disturbances, we will show the sensitivity function of the system.

These shown are the transfer Function which have as input a different disturbance and as output the position of the steel strip, after all disturbances.

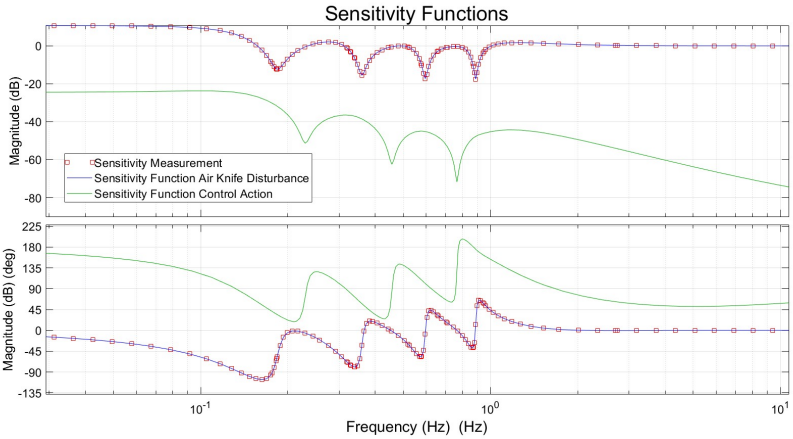

Figure 6.4: Sensitivity Function of the system

- $S_{Measurement}$ is the sensitivity function of the system with the measurement noise as input.
- $S_{AirKnife}$ is the sensitivity function of the system with the air knife as input.
- $S_{Control}$ is the sensitivity function of the system with controller signal as an input.

For $S_{F_{airknife}}$ and $S_{F_{pole}}$ we can see that the system is attenuated only along the natural frequencies, while other frequencies are not attenuated or not much at all.
This shows that the disturbances from both the measurement and the air knife are correctly managed and kept within a certain threshold.
To show in example how this can work, let us consider the same system but with a different source, in this case a signal outside the natural frequencies of the system.

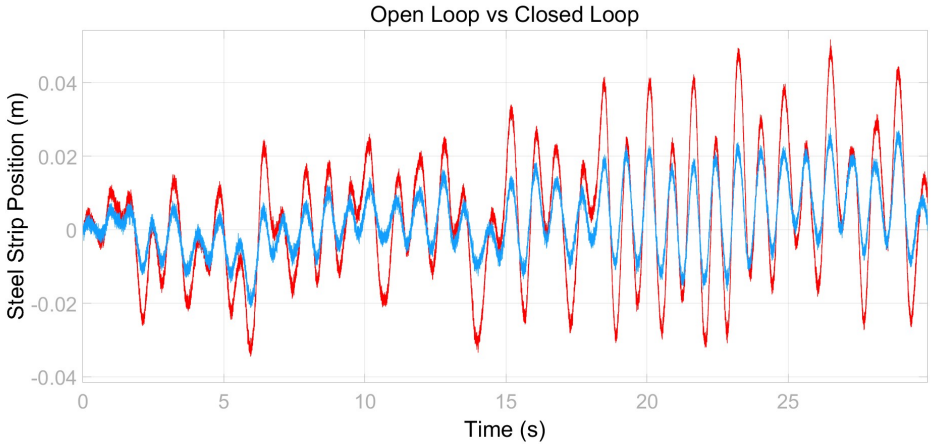

Figure 6.5: Open Loop | Closed Loop

Peaks (Natural Frequencies)	1	2	3	4
Air Knife	0.36	0.595	0.889	1.24
Electromagnetic Actuators	0.184	0.36	0.595	0.889

Table 6.1: Natural Frequencies of the FRFs

6.2. Simulation

In the following figure we can see the result of a simulation of the system with the controller. The same system has been perturbed by 2 different types of disturbances: a white noise and a chirp signal. This last one is chosen to show how the system behaves at different frequencies: The chirp signal slowly increases in frequencies from 0 to 10 Hz in 1000 seconds. We are showing only the first 200 since they are the more relevant for the system.

First let us remember the transfer function of the sys3835, associated to the air knifes:

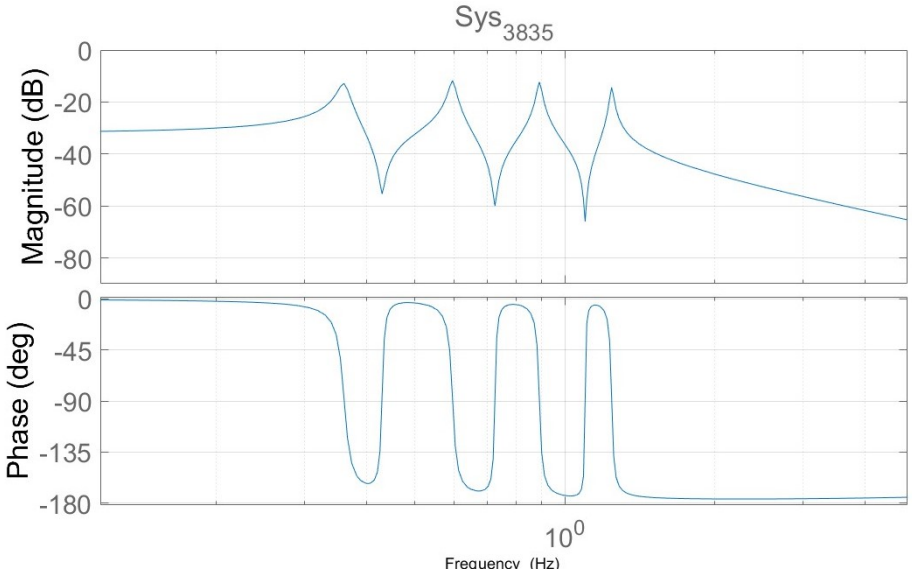

Figure 6.6: Transfer Function of the Air Knifes

And the transfer function of the sys3635, associated to the electromagnetic actuators:

Note that the peaks of the following transfer functions correspond to the natural frequencies of the system:

The chirp signal slowly increases in frequencies from 0 to 10 Hz in 1000 seconds. We are showing only the first 200 since they are the more relevant for the system. So at time 100 seconds the chirp signal is at 1 Hz, at time 200 seconds the chirp signal is at 2 Hz and so on.

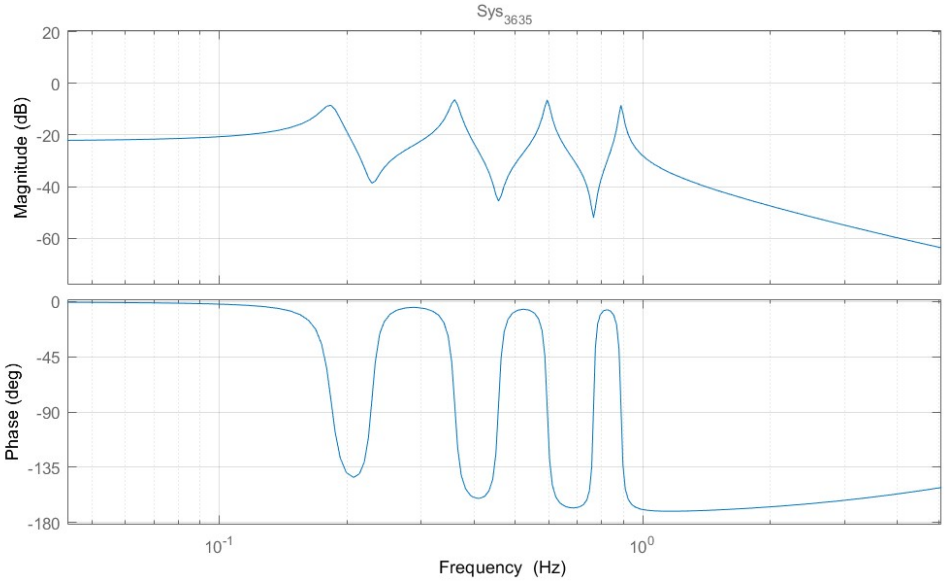

Figure 6.7: Transfer Function of the Electromagnetic Actuators

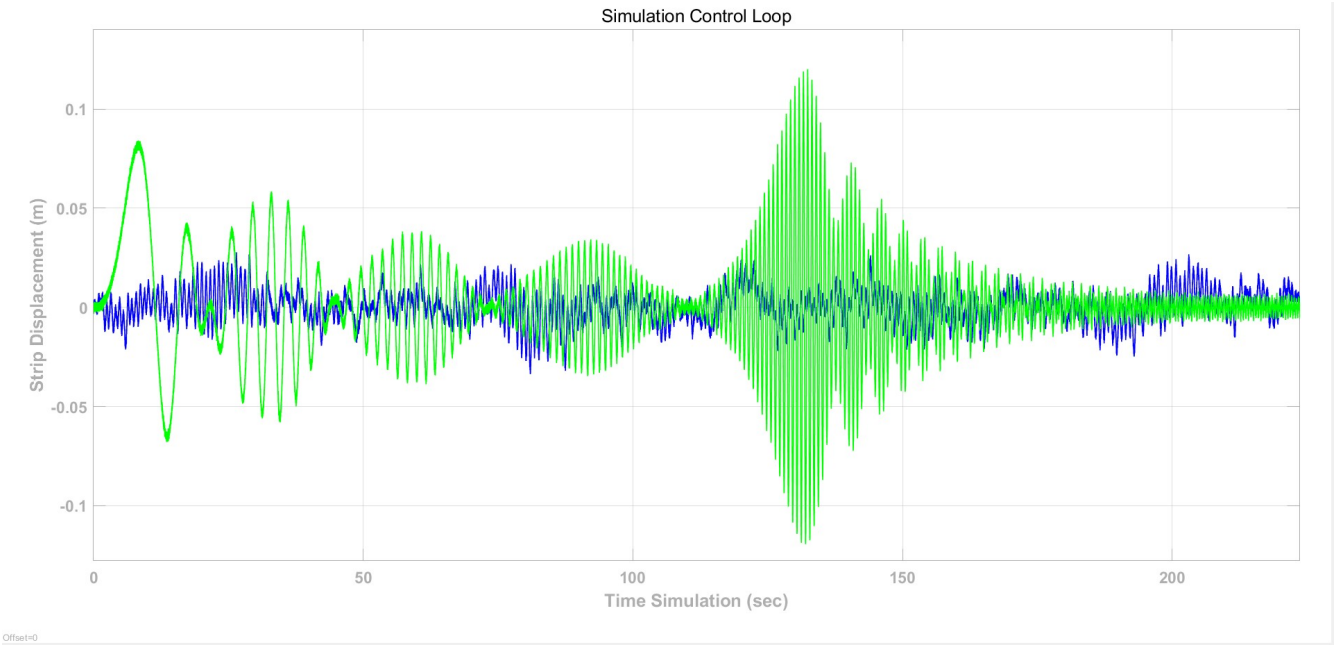

Figure 6.8: White Noise | Chirp

- At the following frequencies: **0.595 Hz** and **0.889 Hz** both the air knife and the electromagnetic actuators are acting on the strip, but the system in closed loop is able to attenuate the displacement.
- At the following frequencies: **1.24 Hz** only the air knife is acting on the strip. Since the air knife is not controlled by the controller, the system is attenuate and the system diverges.

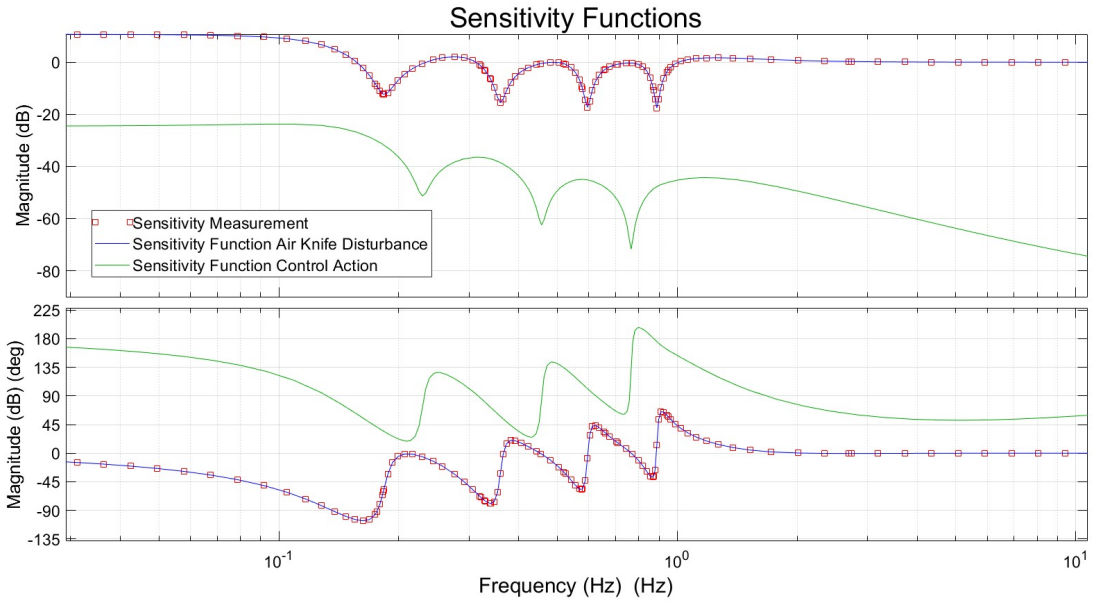

Figure 6.9: Chirp signal

- At the following frequencies: **0.184 Hz** only the electromagnetic system is acting on the strip. The resulting displacement is the effect of a high proportional value of the controller. This suggests to use a lower proportional value for the controller outside the natural frequencies.
- At the following frequencies: **0.229 Hz**, **0.456 Hz**, and **0.776 Hz** the system is almost not disturbed since these frequencies are outside the natural frequencies of the strip, showing how this control system is designed to work on them. These frequencies correspond to the valleys of the sensitivity function associated to the control action.

In conclusion, this Simulation shows how the system is able to attenuate the displacement of the strip at the natural frequencies, while not attenuating the displacement at other frequencies. This is possible thanks to the pole placement controller, which modifies the damping ratio of the natural frequencies, while leaving the other frequencies unchanged.

7 | Conclusions and future developments

7.1. Conclusions

The overarching aim of this work was to establish a user-friendly tool for efficiently simulating and predicting the behavior of strips made from various materials, with different lengths and widths. In this thesis, a new mathematical model has been developed to predict the vibrations of a steel strip during the hot-dip process. The primary goal of this work was to devise a system for simulating the transverse position of the steel strip and to formulate a control scheme for the steel strip system.

The control scheme, implemented using the pole placement algorithm, yielded satisfactory results. It effectively dampened vibrations in the steel strip at specific frequencies while leaving the others largely unaffected. Simulations demonstrated that the closed-loop system significantly reduce vibrations compared to an open-loop system with no controller. Additionally, the system exhibited the ability to act selectively when disturbances match the identified natural frequencies of the steel strip.

We introduced a novel approach for modeling and obtaining the Frequency Response Function of the steel strip. This method, grounded in the Finite Element Method, enabled the acquisition of the FRF at various positions across the width of the steel strip. The effectiveness of this method was validated using data from an industrial plant, and the simulation results were deemed satisfactory.

7.2. Future Work

Potential future work in this research domain will involve the development of a more complex model intended to simulate the behavior of the steel strip more accurately. A two-dimensional Frequency Response Function model will be explored, accounting for

the width and the thickness of the steel strip. This enhanced model will also consider other modes of strip vibrations, such as twisting and flapping, which were not explicitly addressed in this thesis but are present in the steel strip. The proposed system could leverage data from all eight sensors across the width of the strip, providing a more comprehensive understanding of the strip's dynamics.

Another future direction could be using the Virtual Reference Feedback Tuning to estimate a nonlinear system for steel strips. This approach was not considered initially because the data provided did not meet the assumptions necessary for employing this technique.

Given the substantial amount of data available, one natural step will to use all the data available to estimate the system. By employing a data-driven control method to estimate a control model using the u-RLS-3 method, to predict the strip's future position.

A data-driven approach proves to be particularly effective in more accurately predicting nonlinear systems when abundant data is available, as is the case here. Moreover, this approach offers the advantage of estimating the system without relying on a complete mathematical model, which is advantageous in scenarios where the mathematical model of the steel strip is either unknown or incompletely known.

Another promising future direction in the realm of simulating mechanical systems with a plug-and-play approach is the system developed by Professor Gianni Ferretti and Bruno Scaglioni, as outlined in [3]. This system utilizes Modelica or also Dymola using an acausal approach, making modifications and setups easy without the need to compute equations or transfer functions for each modification. This system excels in handling open-chain mechanical systems with ease.

Bibliography

[1] G. Ferretti, L. Bascetta, and P. Rocco. Digital Pole Placement control of multi-mode flexible arms. *2006 ANIPLA International Conference on Methodologies for Emerging Technologies in Automation*. 2006.

[2] M. Saxinger, L. Marko, A. Steinboeck, and A. Kugi. Feedforward control of the transverse strip profile in hot-dip galvanizing lines. *Journal of Process Control*, 92:35-49, 2020. ISSN 0959-1524. DOI: https://doi.org/10.1016/j.jprocont.2020.05.007. URL: https://www.sciencedirect.com/science/article/pii/S0959152420302146. Keywords: Distributed-parameter system, Model-based control, Feedforward control, Steel industry, Hot-dip galvanizing line, Electromagnetic strip stabilizer, Zinc coating.

[3] G. Ferretti, B. Scaglioni, and A. Rossi. Multibody Model of a Motorbike with a Flexible Swingarm. In *Proceedings of the Year Conference*, 2014, March. DOI: https://doi.org/10.3384/ecp14096273.

[4] S. Gaignard and M. Dubois. Characterization of strip vibration at the wiping nozzles. *Metallurgical Research & Technology*, 102(1):83–91, 2005. DOI: https://doi.org/10.1051/metal:2005158.

[5] B. Gospodarič, D. Vončina, and B. Bučar. Active electromagnetic damping of laterally vibrating ferromagnetic cantilever beam. *Mechatronics*, 17(6):291-298, 2007. ISSN 0957-4158. DOI: https://doi.org/10.1016/j.mechatronics.2007.04.002. URL: https://www.sciencedirect.com/science/article/pii/S0957415807000347. Keywords: Active damping, Modal mode, Electromagnet, Vibration of mechanical structures, Current amplifier.

[6] M. Saxinger, L. Marko, A. Steinboeck, and A. Kugi. Active rejection control for unknown harmonic disturbances of the transverse deflection of steel strips with control input, system output, sensor output, and disturbance input at different positions. *Mechatronics*, 56:73-86, 2018. ISSN 0957-4158. DOI: https://doi.org/10.1016/

j.mechatronics.2018.10.008. URL: https://www.sciencedirect.com/science/article/pii/S0957415818301661. Keywords: Distributed-parameter system, Disturbance rejection, Internal model principle, Periodic signals, Active vibration control, Steel industry.

[7] F. Cheli and G. Diana. Vibrations in Continuous Systems. In *Advanced Dynamics of Mechanical Systems*, pages 241–309. Springer International Publishing, 2015. ISBN: 978-3-319-18200-1. DOI: https://doi.org/10.1007/978-3-319-18200-1_3. URL: https://www.doi.org/10.1007/978-3-319-18200-1_3.

A | Appendix Beam Theory

A.1. Beam Theoretical FRF

If we take a homogenous beam, with a constant cross-section A, bending stiffness EI and density ρ all constant along the length of the beam, and we assume the absence of axial loads. This condition is particular since steel strip are under tension in the real world, but from a vibrational point of view it has been seen that the tension is negligible to compute the resonance frequencies. Also even under dynamic conditions, the beam undergoes always to bending in a plane of symmetry and the sections perpendicular to the axis remain plane.

The bending is assumed to progress on a transverse direction z:

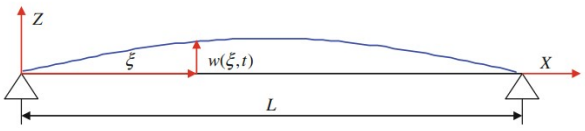

Figure A.1: Transverse Vibrations

The beam, along its length, experiences both internal forces and moments that seek to deform it. These internal forces and moments are contingent upon the deformation of the beam, while external forces and moments are influenced by the position of the beam.

Through some consideration and reasoning, explained more in detail in [7] the following equation represents the motion of a beam under pure bending conditions. It is described via a partial differential equation (PDE). The equation is a fourth-order linear PDE, which is a function of the transverse displacement $w(x,t)$ of the beam:

$$EI\frac{\partial^4 w}{\partial x^4} + \rho A\frac{\partial^2 w}{\partial t^2} = 0 \tag{A.1}$$

which transformed and expanded becomes:

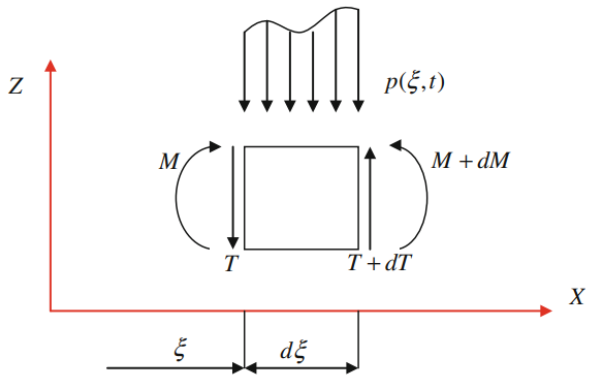

Figure A.2: Internal Forces and Moments which act on a section ξ of the beam

$$w(x,t) = [A\cos(\gamma x) + B\sin(\gamma x) + C\cosh(\omega x) + D\sinh(\omega x)] \cdot \cos(\omega t + \varphi) \tag{A.2}$$

with $\gamma = \sqrt[n]{\frac{\rho A \omega^2}{EI_z}}$

This equation needs to be specified for each different boundary condition. The boundary conditions will affect the natural equations ω for the system and the corresponding mode shapes, while only the initial configurations. Each of the coefficients A, B, C, D can be determined by the initial conditions of the system and how it is excited. We need two conditions for each of the two boundary conditions. Since we are working on a long beam with individual elements limited by 1 meter length the actual beam as a series of smaller elements, which are connected to each other via various conditions.

We will consider the beam to be fixed at the extremities, since the endpoints of the steel strip can't move and are located on rollers which are immobile in their position or can move slightly, while the interconnections between the elements are free to move.

While this explains the position of any point along the beam given an input force, we need to consider the modal approach to compute the resonance frequencies of the system. So the displacement of every point of the beam is computed for each mode of vibration, and the total displacement is the sum of the modal displacements.

$$w_n(x,t) = \sum_{k=1}^{\infty} B_{nk} \sin(\frac{k\pi}{L}x) \cdot \cos(\omega_n t + \varphi_n) \tag{A.3}$$

A.2. Plotting and Computing FRF

Input: Force $F_c e^{i\Omega t}$ applied on the steel strip at applied in C, a point along the beam.

Output: **W** in D, a point along the beam.

Let's express the transverse displacement and the force applied on the as complex variables as a function of time and modal coordinates.

$$\partial W = \partial W^T(x_c, t) \tag{A.4}$$

$$F(t) = \partial q^T \tag{A.5}$$

$$\Phi(x_c) = \partial q^T F_c e^{i\Omega t} \tag{A.6}$$

$$\overline{m}\ddot{q}_i + \overline{c}\dot{q}_i + \overline{k}q_i = \Phi_i(x_c) F_c e^{i\Omega t} \tag{A.7}$$

Resulting in the complex amplitude of the i_{th} mode modal coordinate:

$$q_{i0} = \frac{\Phi_i(x_c) F_c}{-\Omega^2 \overline{m}_{ii} + i\Omega \overline{c}_{ii} + \overline{k}_{ii}} \tag{A.8}$$

The current mode displacement:

$$W_{i0} = \Phi_i(x_0) q_i(0) \tag{A.9}$$

Summing all the modes of the system, we can compute the displacement of the steel strip at any point in time.

$$W_D = \sum_{i=1}^{\infty} W_{i0} = \sum_{i=1}^{\infty} \Phi_i(x_0) q_i(0) \tag{A.10}$$

This Frequency Response Function was obtained by applying 1 Newton of force on the steel strip at point C, and measuring the displacement at point D.

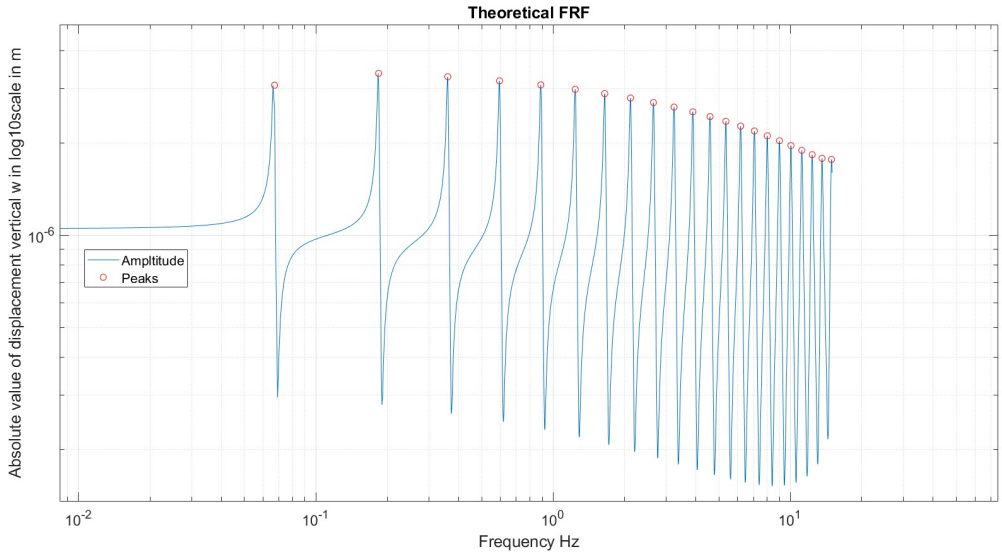

Figure A.3: Theoretical Frequency Response Function of a beam

List of Figures

List of Tables

B | Acknowledgements

I would like to thank first and foremost both my parents and my brother, for their constant patience and tolerance towards my stubborn decisions. To my grandparents and relative family who never showed any doubt in my abilities and always supported me.

Deepest gratitude to my Supervisor and Professor Gianni Ferretti, for his guidance in directing my research and giving me feedback on my work and progress, and giving me the freedom to explore my own ideas. Also for the support and encouragement in some moments of doubt and lost direction.

For all the support and mentorship during my stage in Danieli, I extend my appreciation to all the community for creating such a welcoming environment and making me feel at home. In particular to my academic Supervisor Francesconi Valerio, for his guidance and patience in teaching me the ropes of the industry and inside of the company. For all those little feedbacks and replies to every question, big or small. To Lorenzo Brunato and Giulia Da Pra for the countless coffee breaks. To Andrea Polla and Stefano Martinis for giving me the opportunity to work on this project inside the company. To Marco Mauri, for giving me tips and suggestions for unorthodox approaches and solutions.

Special thanks also to my overseas mentor, Professor Isabella Velicogna, for her ideas and suggestions on how to approach problems and possible future works.

This journey has been a rollercoaster of ups and downs, between finding solutions and getting stuck.